



Minor thesis
in
Theoretical Physics

**Two-dimensional critical phenomena,
interfaces, scaling limits,
and Schramm-Loewner evolutions**

Eveliina Peltola
2016

Advisor: Esko Keski-Vakkuri

HELSINGIN YLIOPISTO
FYSIIKAN LAITOS

PL 64 (Gustaf Hällströmin katu 2)
00014 Helsingin yliopisto

CONTENTS

1. Introduction	3
2. Statistical mechanics, phase transitions and critical phenomena	4
2.1. Boltzmann distribution	5
2.2. First example: the Ising model	6
2.3. Phase transitions and critical phenomena	7
2.4. Ferromagnetic phase transition	8
2.5. Universality	10
3. Examples of discrete models	10
3.1. Percolation	11
3.2. Interfaces	12
3.3. Fortuin-Kasteleyn representation of the Ising model	13
3.4. Potts model	14
3.5. Fortuin-Kasteleyn model	16
3.6. $O(n)$ models	17
4. Critical interfaces in statistical physics	20
4.1. Domain Markov property	21
4.2. Conformal invariance	23
5. Schramm-Loewner evolutions	23
5.1. Riemann mapping theorem	24
5.2. Loewner evolutions	24
5.3. Schramm-Loewner evolutions	26
5.4. Schramm's argument	27
5.5. Phase transition in κ	28
5.6. $\kappa \leftrightarrow 16/\kappa$ duality	28
5.7. Reversibility	29
5.8. Cardy's formula for crossing probabilities	29
6. Restriction properties of SLE_κ	31
6.1. Locality of SLE_6	32
6.2. Restriction property of $SLE_{8/3}$	34
6.3. Brownian exterior perimeter	34
References	36

1. INTRODUCTION

Under certain conditions, systems in nature exhibit phase transitions: drastic changes of thermodynamical states into another. The most familiar example is the phase transition of water from liquid to gas, or solid to liquid. In some cases, when the point of phase transition is approached, the distinctive features of the coexisting phases disappear and the substance is in a homogeneous thermodynamic state. In the vicinity of such a critical point, special kind of phenomena, called *critical phenomena*, happen: the appearance of large fluctuation correlations, self-similarity (resulting in scale invariance in the continuum limit), and power law behavior of thermodynamical functions. The power laws are described by so called *critical exponents*, which are believed to be *universal*, i.e., independent of the microscopic details of the phase transition. The description of phase transitions and critical phenomena as well as the understanding of universality are major aims in thermodynamics and statistical physics.

The scale invariance of critical systems has been studied in terms of the *renormalization group*, the breakthrough of Kenneth G. Wilson who received the Nobel Prize in Physics in 1982 “for his theory for critical phenomena in connection with phase transitions”. Critical systems can be characterized as fixed points in the renormalization group flow. This also explained the emergence of universality. Furthermore, in the 1970s-1980s, Belavin, Polyakov, and Zamolodchikov suggested that the continuum limits of critical systems enjoy not only scale invariance, but also *conformal invariance* which, in the case of two dimensions, is an infinite-dimensional symmetry leading in many cases to exact solvability.

The two-dimensional case is special not only because of the infinitely many conserved quantities but also since the theory of complex analysis provides one with powerful and elegant tools to deal with conformally invariant systems. Furthermore, in the 1920s, a discrete version of complex analysis was developed, and this theory was revived twenty years ago when mathematicians started to rigorously study the concept of conformal invariance and scaling limits of critical systems of statistical mechanics.

In this thesis, we concentrate on geometrical properties of two-dimensional critical systems. We discuss discrete models which can be described using *interfaces*: lattice paths and loops. Remarkably, continuum limits (i.e., scaling limits) of critical interfaces are described by (now quite well-studied) conformally invariant random curves known as (variants of) *Schramm-Loewner evolutions* (SLE) and *conformal loop ensembles* (CLE). In this thesis, we concentrate on *chordal* interfaces connecting boundary points, which are related to so called chordal Schramm-Loewner evolutions (SLE_κ). The introduction of these random conformally invariant curves by Oded Schramm around 2000 was the starting point of a successful interplay between probability theory, stochastic analysis, complex analysis, and more traditional methods of statistical mechanics, such as combinatorics and algebraic methods.

The approach of dealing with critical phenomena in terms of geometric descriptions is nothing new per se. The Coulomb gas approach developed in the 1980s already used geometric ideas to very successfully (but non-rigorously) derive results about two-dimensional critical systems, both in parallel and complementary to those of the field theoretic approach. However, the new approach of the SLE theory that emerged after Schramm’s invention focused on the properties of a single curve describing a random interface in the continuum which could be described by a tractable dynamical growth process called a *Loewner evolution*. In the mathematics literature, such growth process were already studied in the 1920s, by Charles Loewner in terms of complex analysis. The groundbreaking ideas of Schramm was to combine Loewner’s theory with probability, and take the ubiquitous *Brownian motion* as the starting point of the dynamical description of the random growth processes.

The approach started from Schramm’s observations has lead to remarkable success both in physics and mathematics. For instance, conformal invariance of the scaling limits of percolation, the Ising model, and some other models have been established, exact values of critical exponents in many models have been solved, and features of universality have been detected. In particular, results can now be derived directly in the continuum for models for which the traditional lattice methods have failed.

The geometrical approach sheds also new light on critical phenomena and, in particular, their description via *conformal field theory* (CFT). For instance, in the CFT description of the $O(n)$ model, the hitting

points of the interfaces of the boundary of the domain correspond to insertions of boundary changing operators, whose correlation functions satisfy linear second order partial differential equations. On the other hand, these equations are directly related to the Fokker-Planck type equations that arise from the Brownian process describing the growth of the interface in SLE theory. In particular, SLEs are closely related to operators in CFT, and also the conformal anomaly (central charge of CFT) has its counterpart in the theory of SLEs, also showing hints of universality and certain duality relations.

Organization. We begin this thesis by recalling some basics about statistical mechanics in Section 2, with emphasis on continuous phase transitions and critical phenomena, the traditional example of which is the Ising model. Such critical behavior results in self-similarity and scale invariance, leading to the hypothesis of conformal invariance for critical systems. In Section 3, we give various examples of discrete models of statistical mechanics which exhibit critical behavior. The common theme in our presentation is that all the models can be realized in terms of interfaces: lattice paths and loops. The interfaces have an important memorylessness property called the *domain Markov property*. At criticality, also the interfaces exhibit self-similar (fractal) behavior, and in the continuum limit, they are expected (and in some cases rigorously proven) to become conformally invariant. We concentrate on two-dimensional systems where significant progress has been made. In Section 4, we discuss properties of the interfaces in more detail.

In Section 5, we define the Schramm-Loewner evolutions (SLEs) — random curves in the plane which enjoy two natural properties: conformal invariance and the domain Markov property. In this thesis, we will consider *chordal* SLEs which are curves connecting two given boundary points. These processes are characterized by a single real parameter $\kappa \geq 0$, and they are often denoted SLE_κ . There are many variants of SLEs which we will not consider here. It should also be mentioned that in Section 3, we describe many discrete loop models whose loops can be described in the continuum limit by similar processes as SLE_κ , called conformal loop ensembles CLE_κ . Also these processes of random loops have conformally invariant law and they enjoy an appropriate domain Markov property.

In the end of Section 5, we list some natural properties of the SLE_κ curves such as the $\kappa \leftrightarrow 16/\kappa$ duality (which is also frequently discussed in the context of discrete models in Section 3), reversibility, and the phase transitions at $\kappa = 4$ and $\kappa = 8$ (the SLE_κ curve is simple when $\kappa \in [0, 4]$, self-touching when $\kappa \in (4, 8)$, and fills the whole space when $\kappa \geq 8$). We then finish Section 5 with a short argument for the famous percolation crossing formula originally¹ found by John Cardy in 1990s, before the theory of SLEs was born. Lastly, Section 6 contains some interesting features of SLEs: locality and restriction properties and the relation with Brownian excursions. These properties have been manifest in the rigorous treatment of the SLE curves as well as in the determination of critical exponents using SLEs.

2. STATISTICAL MECHANICS, PHASE TRANSITIONS AND CRITICAL PHENOMENA

In statistical mechanics, one is interested in physical systems whose states cannot be exactly specified but instead a probability distribution on the space of microscopic states is considered. This approach is practical for instance when studying systems involving a large number of interacting particles (e.g., of order 10^{23}). The possible microscopic states (the state space) are those which correspond to the observed macroscopic state of the system. The macroscopic state is specified by macroscopic thermodynamical quantities such as volume, pressure, and temperature, whereas properties of the system such as the energy, magnetization, etc., are regarded as statistical averages over an ensemble of microscopic states.

Depending on the question at hand, one considers different types of probability distributions (ensembles) on the state space of the system. In fixed volume, there are three common choices known as the microcanonical, canonical, and grand canonical ensembles. These describe systems in thermodynamic equilibrium, having maximal entropy. Maximizing the entropy of the system with a fixed energy and particle number, one is led to consider the *microcanonical ensemble*. In the microcanonical ensemble,

¹We will not discuss the original CFT arguments of Cardy, but instead give an argument that relies on the description of percolation interfaces as SLE_6 curves.

every microscopic state is assigned equal probability to occur. Of course, this does not correspond to an experimentally realistic situation. Therefore, one usually allows for some uncertainty in the energy and/or particle number, and considers instead the canonical or grand canonical ensemble. In the former, the system is in thermal equilibrium with a heat bath at fixed temperature, and in the latter, the system is in thermal and chemical equilibrium with a reservoir.

More precisely, the *canonical ensemble* maximizes the entropy under the constraint that the expected value of the energy of the system is a given constant E . In the canonical ensemble, the number of particles is fixed. On the other hand, the *grand canonical ensemble* is obtained by maximizing the entropy when the expectations of both the energy and the number of particles in the system are given constants E and N . In particular, both the energy and particle number are then *random variables*.

In the canonical ensemble, the energy of the system has Gaussian distribution with variance of order $\Delta E = \mathcal{O}(\sqrt{N})$, where N is the number of particles. As $N \rightarrow \infty$, the energy fluctuations are of order $\frac{\Delta E}{E} = \mathcal{O}(1/\sqrt{N})$ since one expects $E = \mathcal{O}(N)$. Thus, the relative inaccuracy of the energy is very small for a large system. Similarly, the relative inaccuracy of the particle number is of order $\frac{\Delta N}{N} = \mathcal{O}(1/\sqrt{N})$ as well. Therefore, for very large systems (e.g. at the thermodynamic limit), the microcanonical, canonical, and grand canonical ensembles are essentially equivalent. We refer to [Hon06] for details.

Bibliographical comments. Textbooks, lecture notes, and surveys about statistical mechanics, phase transitions, and critical phenomena include (but are certainly not limited to) [Uzu92, Hon06, Bax07, Mus10, Hon13]. Also in the CFT book [DFMS97], statistical mechanics is discussed with a particular emphasis in the hypothesis of conformal invariance at criticality.

2.1. Boltzmann distribution. We shall be interested in systems which are in thermal contact with the environment but the number of particles is fixed. In this case, the probability of the system to be in a given microscopic state σ is given by the *Boltzmann distribution* (the canonical ensemble)

$$\mathbb{P}[\sigma] = \frac{e^{-\beta E(\sigma)}}{Z}$$

where $\beta = 1/T$ is the inverse temperature, $E(\sigma)$ the energy of the state σ , and Z is the *partition function*,

$$Z = \sum_{\sigma} e^{-\beta E(\sigma)}.$$

The (Helmholz) *free energy* of the system is $F = -T \log Z$. It describes the amount of energy that can be converted into work at constant temperature T and volume V . The ensemble average is denoted

$$\langle A \rangle = \frac{1}{Z} \sum_{\sigma} A(\sigma) e^{-\beta E(\sigma)},$$

where $A = A(\sigma)$ is some observable depending on the microscopic state σ . For instance, the average energy is

$$\langle E \rangle = \frac{1}{Z} \sum_{\sigma} E(\sigma) e^{-\beta E(\sigma)} = -\frac{\partial}{\partial \beta} \log Z.$$

Important features of phase transitions and critical phenomena are encoded in the pair correlations

$$C(A, B) = \langle AB \rangle - \langle A \rangle \langle B \rangle$$

of observables A and B . In the *scaling limit* (that is, continuum limit of the model), the correlations of local observables should become correlation functions of local operators in some quantum field theory (QFT). For systems with short-range interactions, the correlations typically have exponential decay in the distance of particles. However, at a critical point (where a continuous phase transition takes place), the correlations have power law behavior (see Sections 2.3 and 2.4 below). At criticality, the scaling

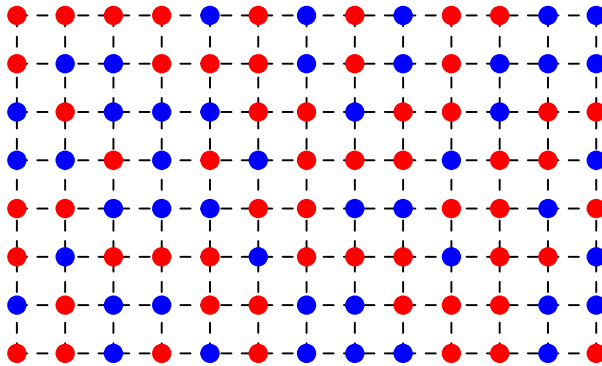


FIGURE 2.1. Configuration of the Ising model on a square lattice. The two colors represent the spins $+1$ and -1 .

limit of the system should be described by a conformal field theory (CFT), that is, a massless QFT with conformal symmetry. In this thesis, we will concentrate on systems in two-dimensions, where the conformal symmetry is infinite-dimensional and, in addition, the powerful tools of complex analysis are applicable.

2.2. First example: the Ising model. The prototypical example of a statistical mechanics model is the Ising model. It was introduced by Wilhelm Lenz in the 1920s, but it is named after Lenz's student, Ernst Ising, who solved the model in the 1920s in the one-dimensional case and noted that no phase transition occurs. This led him to conjecture that the model would have no phase transition in any dimension. The conjecture was shown to be wrong in 1936, when Rudolf Peierls proved the existence of a continuous phase transition in dimensions at least two (see Section 2.4 below). The Ising model has been widely studied ever since. Recently, it was shown by Stanislav Smirnov and his collaborators [Hon10, Smi10, CS12, CI13, HS13, CDCH⁺14, CHI15, Izy16], that in the scaling limit, the critical two-dimensional Ising model (on isoradial graphs) enjoys conformal invariance: the interfaces of the model converge in the scaling limit to Schramm-Loewner evolution type curves (SLE_κ , CLE_κ) with $\kappa = 3$, and the correlations converge to correlation functions of a conformal field theory with central charge $c = 1/2$.

On a finite graph $\mathcal{G} = (\mathcal{V}, \mathcal{E})$ with vertices \mathcal{V} and edges \mathcal{E} , a configuration in the Ising model consists of an assignment $\sigma: \mathcal{V} \rightarrow \{\pm 1\}$ of spins $\sigma_i \in \{\pm 1\}$ to each vertex $i \in \mathcal{V}$. The number of particles in the system is $N = |\mathcal{V}|$. The energy of a configuration σ is given by

$$(2.1) \quad E[\sigma] = -J \sum_{(i,j) \in \mathcal{E}} \sigma_i \sigma_j - h \sum_{i \in \mathcal{V}} \sigma_i,$$

where J is the coupling constant representing the interaction of the spins, and h is the strength of an external magnetic field. The coupling of the spins can be either ferromagnetic ($J > 0$) or antiferromagnetic ($J < 0$). The interaction is of very short range (nearest neighbors only), represented by the edges (i, j) of the graph. In the ferromagnetic coupling ($J > 0$), the Boltzmann distribution favors configurations where the neighboring spins are aligned, and when $h \neq 0$, the spins also tend to be aligned with the external magnetic field.

In the Ising model, the mean value $\langle \sigma_{i_0} \rangle$ of a spin at $i_0 \in \mathcal{V}$ represents the magnetization at that point. Assuming translation invariance, we can write $\sum_i \langle \sigma_i \rangle = N \langle \sigma_{i_0} \rangle$. Therefore, for any i_0 , the magnetization reads

$$(2.2) \quad M := \langle \sigma_{i_0} \rangle = \frac{1}{N} \sum_{i \in \mathcal{V}} \langle \sigma_i \rangle = \frac{1}{NZ} \sum_{\sigma} \sum_{i \in \mathcal{V}} \sigma_i e^{-\beta E(\sigma)} = -\frac{1}{N} \frac{\partial F}{\partial h},$$

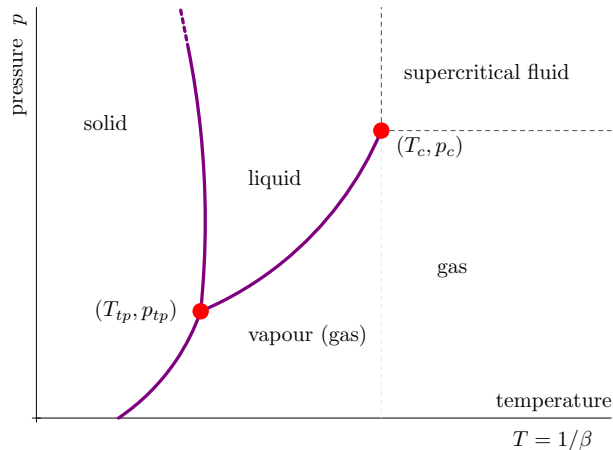


FIGURE 2.2. The phase diagram of water. The liquid-gas, liquid-solid, and solid-gas phase transitions are of first order. At the triple point (T_{tp}, p_{tp}) , all three phases water coexist. At the critical point (T_c, p_c) , there is a continuous phase transition.

where $F = -T \log Z$ is the free energy. Another feature of interest is the magnetic susceptibility

$$\begin{aligned}
 (2.3) \quad \chi &:= \left. \frac{\partial M}{\partial h} \right|_{h=0} = \frac{1}{N} \left. \frac{\partial}{\partial h} \left(\frac{1}{Z} \sum_{\sigma} \sum_{i \in \mathcal{V}} \sigma_i e^{-\beta E(\sigma)} \right) \right|_{h=0} \\
 &= \frac{1}{NT} \left(\left\langle \left(\sum_i \sigma_i \right)^2 \right\rangle - \left\langle \sum_i \sigma_i \right\rangle^2 \right) \\
 &= \frac{1}{NT} \text{Var} \left(\sum_i \sigma_i \right).
 \end{aligned}$$

It describes how the system responds to a very small external magnetic field. The above calculation shows that the susceptibility is proportional to the variance of the total spin of the system.

Both the magnetization and the magnetic susceptibility can be expressed in terms of derivatives of the free energy, so the knowledge of the free energy F , or equivalently, of the partition function Z , is of crucial importance. In 1944, Lars Onsager managed to calculate explicitly the free energy of the two-dimensional Ising model (on the square lattice), using a transfer matrix method. The three-dimensional case still remains open — the Ising model in dimensions four and more agrees with its mean field theory (i.e., the upper critical dimension is four), and the one-dimensional case was solved already in the 1920s.

2.3. Phase transitions and critical phenomena. Under certain conditions, systems in nature exhibit phase transitions. Then, in the space of the macroscopic states of the system (spanned by the thermodynamic variables), there are several different homogeneous regions (i.e., *phases*) where the macroscopic system is at equilibrium. For instance, water has essentially² three phases in nature: liquid, solid (= ice), and gas. In the (T, p) -plane, T being temperature and p pressure, there is a triple point $(T_{tp}, p_{tp}) = (0.01^\circ\text{C}, 610 \text{ Pa})$ where all three phases coexist. This point is the intersection of the liquid-gas and liquid-solid coexistence curves — see Figure 2.2. The liquid-gas coexistence curve ends at the critical point $(T_c, p_c) = (374.15^\circ\text{C}, 22 \text{ MPa})$.

To distinguish the two phases in a phase transition, one associates to the transition an *order parameter*, that is, a physical quantity which is zero in one phase and assumes non-zero values in the other phase. For instance, in the gas-liquid transition, a natural choice of the order parameter is the difference between

²In principle, also supercritical fluid can occur, but this only happens in specific conditions: in very high temperature and pressure.

the densities of liquid and gas. As another example, magnetization serves as the order parameter in the phase transition of the ferromagnetic Ising model (see Figure 2.3 and Section 2.4). If the order parameter is continuous across the phase transition, the phase transition is said to be *continuous*, and otherwise it is called a *first order (discontinuous) phase transition*. For instance, in the phase diagram of water (see Figure 2.2), at the coexistence curves, first order phase transitions take place, except at the critical point, where the phase transition becomes continuous (second order in Ehrenfest classification).

In this thesis, we will concentrate on systems with continuous phase transitions, which are related to conformal invariance. Points of continuous phase transitions are called *critical points*. Near the critical point, the system can exhibit long-range interactions even though the physical interactions are a priori of very short range. At criticality, the interactions typically become of infinite range (if the correlation length diverges). Critical systems thus exhibit self-similar behavior, and in the continuum limit, they become scale invariant and thus fixed by the renormalization group flow [PP66, Kad66, Kad90, Car96]. A further symmetry, conformal invariance, was postulated in the 1970s-1980s by Belavin, Polyakov, and Zamolodchikov [Pol70, BPZ84a, BPZ84b], see also [DFMS97].

In continuous phase transitions, the order parameter, free energy, and various response functions and correlation functions typically exhibit non-analytic behavior³ as functions of the thermodynamic variables⁴. This behavior usually displays itself in the form of power law singularities or decay in the distance from the critical point, e.g., behavior of the type $|T - T_c|^{\pm\vartheta}$ with $\vartheta > 0$. For instance, in the case of the Ising model, the magnetization exhibits such a behavior with $\vartheta = 1/8$ (see Section 2.4 below). The exponents ϑ appearing in such power laws are called the *critical exponents* of the phase transition.

2.4. Ferromagnetic phase transition. Rudolf Peierls proved in 1936 that the ferromagnetic Ising model ($J > 0$) in dimension at least two has a continuous phase transition: in low temperatures, the system exhibits spontaneous magnetization, but not in high temperatures — see Figure 2.3. The phase transition occurs at a unique critical temperature $T_c = 1/\beta_c$, such that the magnetization $M = M_\beta(h)$ defined in (2.2) behaves as follows: for $T < T_c$, we have

$$\lim_{h \searrow 0} M_\beta(h) > 0 \quad \text{and} \quad \lim_{h \nearrow 0} M_\beta(h) < 0,$$

whereas for $T > T_c$, both limits are zero. In dimension two, when $h \searrow 0$, the magnetization is

$$M_\beta(0_+) := \lim_{h \searrow 0} M_\beta(h) \begin{cases} \rightarrow 1 & \text{as } T \rightarrow 0 \\ = m(T) \in (0, 1) & \text{when } 0 < T < T_c \\ \sim |T - T_c|^{1/8} & \text{as } T \rightarrow T_c \\ = 0 & \text{when } T > T_c \end{cases}$$

and it is continuous across the phase transition at T_c . However, its derivative with respect to the magnetic field h (that is, the magnetic susceptibility (2.3)) diverges at the critical point T_c :

$$\left. \frac{\partial M_\beta(h)}{\partial h} \right|_{h \searrow 0} \sim |T - T_c|^{-7/4} \quad \text{as } T \rightarrow T_c.$$

The powers $1/8$ and $7/4$ above are critical exponents of the Ising model. To each thermodynamic function, such a critical exponent is associated, which expresses its power law behavior as $T \rightarrow T_c$.

³Mathematically, phase transitions can only happen in the thermodynamic limit (when $V, N \rightarrow \infty$ so that $\frac{N}{V} = \text{const.}$) since functions defined on finite lattices are always continuous.

⁴Traditionally, phase transitions are classified by these discontinuities (Ehrenfest classification). For instance, the free energy F is continuous as a function of the thermodynamic variables, but its derivatives may have discontinuities or singular behavior. In Ehrenfest classification, discontinuity points of the first derivatives of F are said to be points of a *first order phase transition*, whereas points where the first derivatives of F are continuous but some of the second order derivatives fail to be continuous, are called points of *second order phase transitions*.

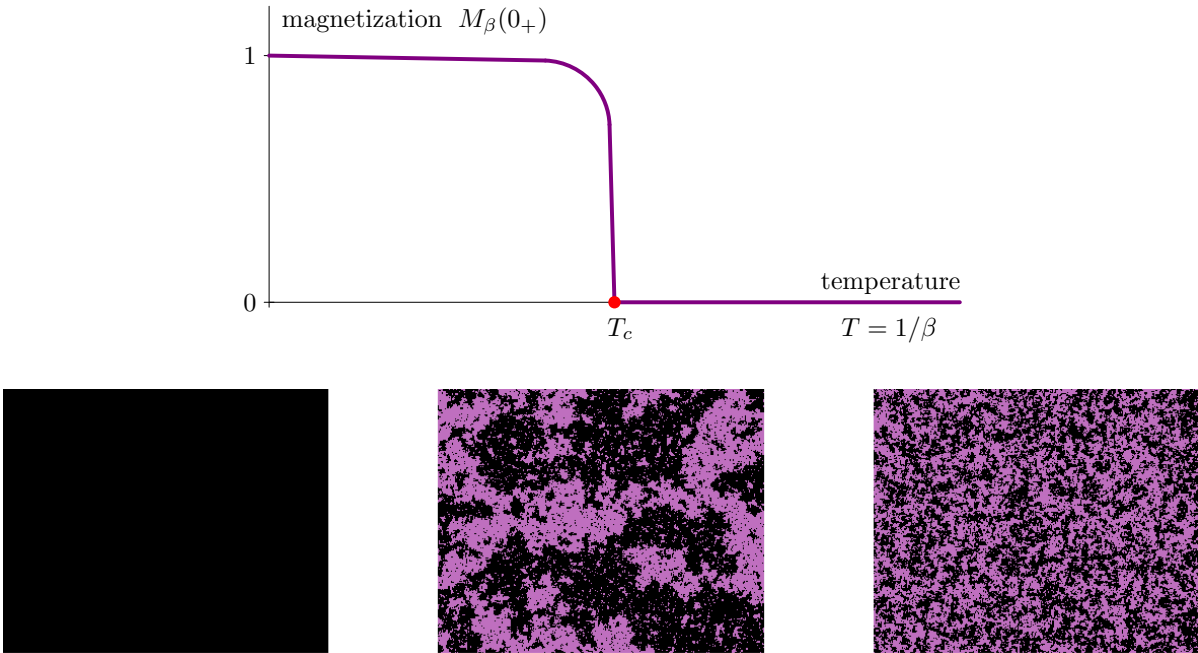


FIGURE 2.3. The phase transition of the ferromagnetic ($J > 0$) Ising model. In high temperatures (right), the system is disordered, and the magnetization of the system is zero, whereas in low temperatures (left), aligned spins are favored, and the magnetization is non-zero. At criticality, macroscopic clusters of aligned spins appear. The magnetization is continuous across the phase transition at T_c .

An important feature of continuous phase transitions is the divergence of the correlation length at the critical point. In the Ising model, the correlation between two spins at i and j is

$$C_\beta(i, j) := \langle \sigma_i \sigma_j \rangle - \langle \sigma_i \rangle \langle \sigma_j \rangle.$$

In off-critical temperatures ($T \neq T_c$), the correlations decay exponentially fast in the distance $|i - j|$:

$$C_\beta(i, j) \sim e^{-\frac{1}{\xi}|i-j|} \quad \text{as } |i - j| \rightarrow \infty,$$

where $\xi = \xi(T)$ is the correlation length. When approaching the critical temperature, long-range fluctuations appear and the correlation length diverges:

$$\xi(T) \sim |T - T_c|^{-1} \rightarrow \infty \quad \text{as } T \rightarrow T_c.$$

Then, the decay of the correlations is only polynomial:

$$C_{\beta_c}(i, j) \sim |i - j|^{-1/4} \quad \text{as } |i - j| \rightarrow \infty.$$

The powers 1 and 1/4 are the critical exponents associated to the correlation length and the spin correlations, respectively. The above values of the critical exponents are given for the case of dimension two. Thanks to the exact solvability of the two-dimensional Ising model, the values of all its critical exponents are known, whereas in the three-dimensional case, only numerical values have been obtained (the three-dimensional Ising model has not been exactly solved!). In dimension at least four, all the critical exponents are also known exactly because the model agrees with its mean field theory.

In continuous phase transitions, spontaneous symmetry breaking can take place. For instance, in the phase transition of the ferromagnetic Ising model, the material in the paramagnetic phase (above the critical temperature, disordered phase) is rotationally symmetric and, whereas in the ferromagnetic phase (below the critical temperature, ordered phase), there is a preferred direction of the total magnetization of the matter (in alignment with the external magnetic field), breaking the global rotational symmetry.

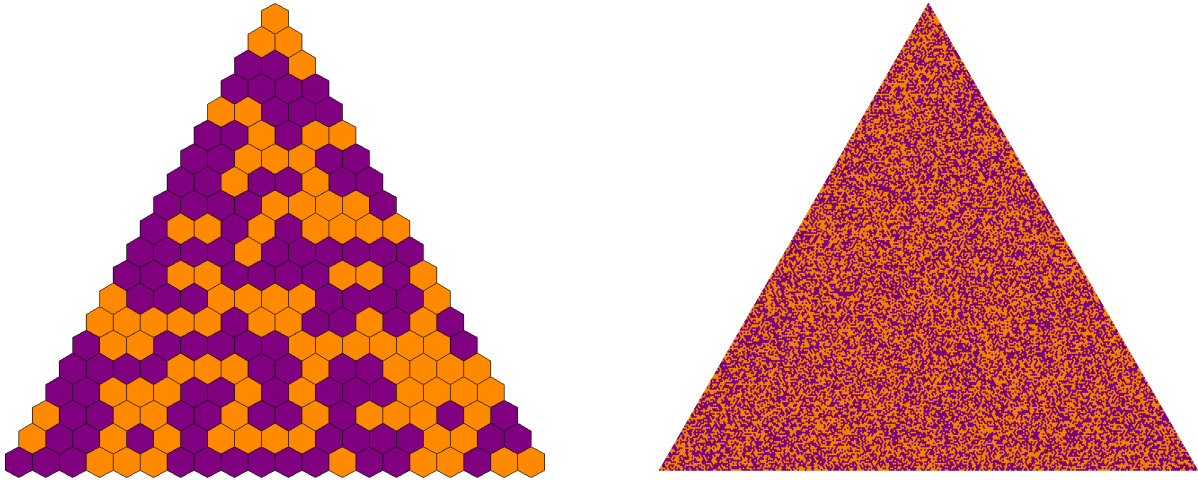


FIGURE 3.1. Samples of critical percolation configurations on faces of the hexagonal lattice, in equilateral triangles with side lengths 20 (left) and 300 (right).

2.5. Universality. Continuous phase transitions are largely insensitive to microscopic properties of the system. In particular, such phase transitions can often be described by global properties of the system only: the spatial dimension and the internal symmetry of the order parameters. This phenomenon is called *universality* of continuous phase transitions. One speaks of different universality classes and many microscopically different systems can exhibit similar behavior at their critical point, thus belonging to the same universality class. For instance, the values of the critical exponents of the phase transition are found to coincide quite accurately for systems in the same universality class. Universality gives an important tool to analyze systems with continuous phase transitions: one can pick one's favorite model from the universality class, according to which model is the easiest to analyze for the question at hand.

At the critical point, the scaling limits of models in the same universality class should be described by a similar conformal field theory, and the critical interfaces should be described by conformally invariant random curves such as the ones studied in this thesis, characterized by a single real parameter, $\kappa \geq 0$. This parameter is related to the conformal anomaly number of the CFT via $c(\kappa) = \frac{1}{2\kappa}(\kappa - 6)(8 - 3\kappa)$.

3. EXAMPLES OF DISCRETE MODELS

In this section, we give examples of planar lattice models which exhibit critical behavior (undergo continuous phase transitions) and can be described using *interfaces*: random non-intersecting lattice paths and loops. Remarkably, continuum limits (i.e., scaling limits) of such critical interfaces are described by conformally invariant random curves known as (variants of) Schramm-Loewner evolutions (SLE) and conformal loop ensembles (CLE).

Bibliographical comments. Exactly solvable models in statistical mechanics have (naturally) been widely studied, and there are many surveys about them. In the books [Uzu92, Bax07, Mus10], many models discussed below in this section are treated in detail. The book [Smi02] gives a more quantum field theoretical approach. The lecture notes [KN04, Car05, BB06, Dup06, HKB⁺12] have a particular emphasis on conformal invariance and the description of the models via interfaces — as will be our viewpoint, too.

The models we treat in this thesis have received quite a lot of interest from mathematicians as well, and many rigorous results have been obtained (relatively recently). Mathematical introductions to critical discrete models include [Gri99, Wer06, Gri09], and a very nice survey about critical behavior especially in the Fortuin-Kasteleyn (random cluster) and $O(n)$ models is presented in [DC11].

3.1. Percolation. Percolation theory has been used e.g. in the study of disordered media. Hammersley and Broadbent defined a percolation model in 1957, in order to study how the random properties of a medium influence the percolation of a fluid through it — in contrast with the so far conventional approach of diffusion theory, where the random properties of the fluid were emphasized. Remarkably, the same model has several interpretations: in addition to the diffusion of fluid, molecules, electrons, etc., with percolation one can study e.g. spreading of infectious diseases. It also provides a simplified model for the study of interacting random systems.

Consider a hexagonal lattice \mathcal{G} on the plane⁵. In a simple percolation model, one colors the faces of \mathcal{G} with two colors with equal probability — that is, each site has probability $1/2$ to be colored yellow and $1/2$ to be colored purple, say. Thus, a configuration in this percolation model is a coloring of the faces (hexagons) of the graph \mathcal{G} , as illustrated in Figure 3.1. This model, simple as it may be, displays quite interesting features. In particular, it is critical and has a conformally invariant scaling limit.

Criticality of the percolation model can be seen when modifying the probabilities to color the faces with the two colors. Suppose that, instead of the fifty-fifty chance, each face has probability p to be colored yellow and $1 - p$ to be colored purple. Then, if $p > 1/2$, there should be more yellow faces in a typical configuration, and if $p < 1/2$, more purple ones. This observation can be quantified as follows. Consider the probability of the event A that, in the continuum limit, in the percolation configuration there is an infinite cluster (i.e., connected component) of yellow hexagons. The percolation model exhibits a phase transition at $p_c = 1/2$ in the following sense: when $p > 1/2$, the probability of the event A equals one, whereas in the case $p \leq 1/2$, the probability of A equals zero, almost surely — see e.g. [Kes82, Gri99]. Moreover, in the case $p > 1/2$, the infinite yellow cluster is almost surely unique.

At the critical point $p_c = 1/2$, no infinite yellow cluster exists. As $p \searrow p_c$, the probability that the origin belongs to the infinite cluster behaves as follows:

$$\mathbb{P}[0 \text{ belongs to the infinite yellow cluster}] \sim |p - p_c|^{5/36}.$$

This power law behavior was rigorously proven (for percolation on faces of the hexagonal lattice) in [SW01] by Smirnov and Werner, using new methods relying on the convergence of critical interfaces to SLE type curves, defined in Section 5. Other examples of rigorously known values of the critical exponents (also for the hexagonal lattice) include⁶

- [SW01]: the average size of finite clusters, which behaves as $|p - p_c|^{-43/18}$
- [SW01]: the correlation length (the typical radius of a finite cluster), which behaves as $|p - p_c|^{-4/3}$
- [LSW02b]: the probability that the cluster containing the origin has diameter larger than R , which decays like $R^{-5/48}$ as $R \rightarrow \infty$.

The analogy of the free energy for percolation is the cluster density, that is, the average number of clusters per site. It is believed to behave as $|p - p_c|^{2-\alpha}$ (it is conventional to denote the exponent in two dimensions by $2 - \alpha$), where the critical exponent is $\alpha = -2/3$. To prove this, however, remains an open problem.

The above values of the critical exponents are given in dimension two. The upper critical dimension of percolation is six, and mean field theory thus gives the critical exponents in dimensions at least six. However, in dimensions between three and five, only numerical results have been obtained. As already mentioned, there are still open questions concerning the two-dimensional case, too, but at least exact predictions can be made using CFT and Coulomb gas arguments, for instance.

As the universality hypothesis suggests, the critical exponents are believed to be independent of the chosen lattice. On the other hand, the value of the critical point p_c is highly dependent of the lattice,

⁵The percolation model can of course be defined on any graph in any dimension, but the scaling limit has been (so far) understood mathematically only in two dimensions (in the case of faces of the hexagonal lattice and sites on its dual lattice, the triangular lattice). Also, exact values of the critical point and critical exponents are known in these cases.

⁶Also in the series of articles [LSW01b, LSW01c, LSW02c], critical exponents of percolation (and Brownian motion) are studied using SLE techniques.

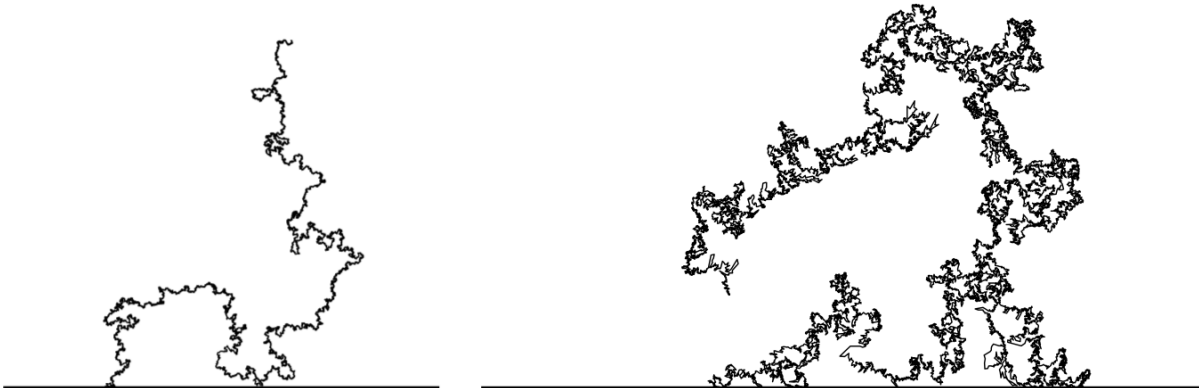


FIGURE 3.2. Illustrations of Schramm-Loewner evolution SLE_κ curves with $\kappa = 3$ (left) and $\kappa = 6$ (right). These SLE_κ curves correspond with interfaces in the critical Ising model ($\kappa = 3$) and critical percolation ($\kappa = 6$), respectively. The curve on the right has self-touchings whereas the one on the left does not. Also, the curve on the right looks rougher and, indeed, its fractal dimension is $7/4 = 1.75$, whereas the fractal dimension of the curve on the left is $11/8 = 1.375$. (©Antti Kemppainen.)

and it has been calculated exactly only for very few sufficiently symmetric lattices. For percolation on the faces of the hexagonal lattice (sites of the triangular lattice), as in Figure 3.1, and on edges (bonds) of the square lattice, we have the very nice value $p_c = 1/2$, see e.g. [Gri99].

3.2. Interfaces. Interfaces separating the yellow and purple hexagons arise naturally in percolation configurations. Because the faces are colored independently, the interfaces only depend on the faces nearby. This property is called locality — see Section 6.1 for details.

The interfaces form closed loops and paths between boundary points. Imposing boundary conditions, one can produce macroscopic interfaces between given boundary points of the lattice. For instance, adding a layer of yellow hexagons on a segment of the boundary and a layer of purple hexagons on the complementary boundary segment, one can define an exploration process by following the interface between the yellow and purple hexagons so that the purple hexagons always lie on the left hand side of the explorer, say. It was rigorously proved by Smirnov [Smi01] that, at critical p_c , this random curve has a conformally invariant scaling limit, the Schramm-Loewner evolution curve SLE_6 (see Section 5). This was the first step towards the proof of complete conformal invariance of critical percolation. In 2010, Smirnov was awarded the prestigious Fields medal for his work⁷ “for the proof of conformal invariance of percolation and the planar Ising model in statistical physics”. The SLE_6 curve is far from smooth — it is a fractal curve of Hausdorff dimension $7/4$, having many self-touchings, as illustrated in Figure 3.2.

More generally, Camia and Newman [CN07, CN06] proved that the loops surrounding the two different colors in critical percolation (in the hexagonal lattice) converge in the scaling limit to SLE_6 type processes called conformal loop ensembles CLE_6 . The value of the parameter $\kappa = 6$ corresponds to a conformal field theory with central charge $c = 0$. The outer boundaries of these percolation interfaces (note that while the curves have self-touchings, their frontiers are simple curves) are described by SLE_κ and CLE_κ type processes with the dual⁸ value $\kappa = 8/3$ — we discuss more about the duality $\kappa \leftrightarrow 16/\kappa$ in Section 5.6, see also [Dup00, Bef04, Dup04, Dub07, Zha08a]. The $SLE_{8/3}$ process should describe the scaling limit of self avoiding random walks, although there is no complete mathematical proof yet. Hence, the outer boundaries of the percolation interfaces should look locally like self avoiding walks.

⁷Also, already in 2006, Wendelin Werner was awarded the Fields medal “for his contributions to the development of stochastic Loewner evolution, the geometry of two-dimensional Brownian motion, and conformal field theory”.

⁸Observe that we have $c(6) = c(8/3) = 0$ and more generally, $c(\kappa) = c(16/\kappa) = \frac{1}{2\kappa}(\kappa - 6)(8 - 3\kappa)$.

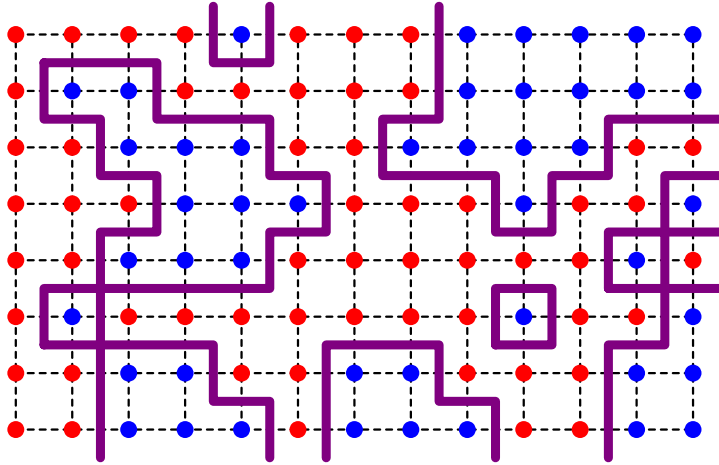


FIGURE 3.3. Configuration of the Ising model on a square lattice. The two colors represent the spins $+1$ and -1 . The domain walls are illustrated in purple.

Similarly as for percolation, one can describe the Ising model in terms of interfaces (these are often called *domain walls*), see Figure 3.3. The Ising model is in fact another example of a model whose interfaces at criticality have been rigorously shown to converge in the scaling limit to SLE_κ and CLE_κ type processes, with $\kappa = 3$ and central charge $c = 1/2$, and in fact, convergence results concerning the dual value $\kappa = 16/3$ are also known [Smi10, CS12, CDCH⁺14, KS15].

In an Ising spin configuration σ on vertices \mathcal{V} of a finite planar graph $\mathcal{G} = (\mathcal{V}, \mathcal{E})$, the domain walls are interfaces that one naturally associates between spins that are not aligned. They are realized as collections of edges of the dual graph \mathcal{G}^* , forming loops and paths between boundary points. The dual graph $\mathcal{G}^* = (\mathcal{V}^*, \mathcal{E}^*)$ of \mathcal{G} consists of vertices \mathcal{V}^* at the centers of the faces of \mathcal{G} and edges \mathcal{E}^* between them crossing the edges \mathcal{E} . To each edge in \mathcal{E} , there is a dual edge in \mathcal{E}^* crossing it.

The domain walls are particularly useful when studying the Ising model at low temperature. We now derive the low temperature expansion of the partition function in terms of the domain walls. Consider the two-dimensional Ising model in zero magnetic field, so that the energy of a spin configuration σ is given by (2.1) with $h = 0$. Let also $J > 0$ (the ferromagnetic case). First, note that the Boltzmann weight of a spin configuration σ is

$$\mathbb{P}[\sigma] = \frac{1}{Z_{\text{Ising}}} \prod_{(i,j) \in \mathcal{E}} e^{\beta J \sigma_i \sigma_j},$$

which shows that in the most likely configurations, all the spins have equal value. Every edge $(i,j) \in \mathcal{E}$ for which $\sigma_i \neq \sigma_j$ results in a factor $e^{-\beta J}$, reducing the probability of the configuration σ . Such edges exactly correspond with the domain walls. The partition function can be written in the form

$$(3.1) \quad Z_{\text{Ising}} = \sum_{\sigma} \prod_{(i,j) \in \mathcal{E}} e^{\beta J \sigma_i \sigma_j} = \sum_{\sigma} e^{\beta J |\mathcal{E}|} \prod_{\substack{(i,j) \in \mathcal{E} \\ \sigma_i \neq \sigma_j}} e^{-2\beta J} = e^{\beta J |\mathcal{E}|} \sum_{\sigma} (e^{-2\beta J})^{\#\{\text{edges in the domain walls}\}}.$$

In low temperature, $\beta \gg 1$ and the factor $e^{-2\beta J}$ is small (the factor $e^{\beta J |\mathcal{E}|}$ in the front is a global universal constant and can be ignored), and therefore, Equation (3.1) is called the low temperature expansion of the Ising partition function. Peierls used (3.1) together with a high temperature expansion (which we will not consider in this thesis) to prove the existence of a continuous phase transition in the two-dimensional Ising model.

3.3. Fortuin-Kasteleyn representation of the Ising model. Consider still the Ising model in zero magnetic field $h = 0$. Using the observation that the interaction of two spins can be written in the form

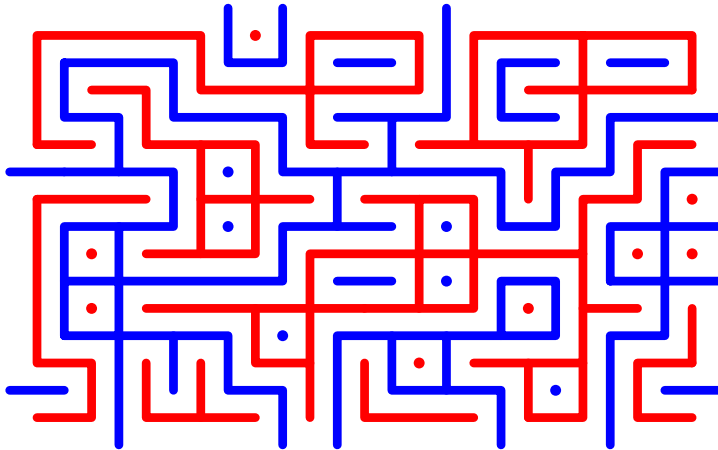


FIGURE 3.4. Fortuin-Kasteleyn clusters \mathcal{G}' (red) and their dual clusters $(\mathcal{G}')^*$ (blue).

$\sigma_i \sigma_j = 2\mathbb{1}_{\{\sigma_i = \sigma_j\}} - 1$, we can write the partition function (3.1) in the form

$$\begin{aligned} Z_{\text{Ising}} &= \sum_{\sigma} \prod_{(i,j) \in \mathcal{E}} e^{\beta J \sigma_i \sigma_j} = e^{-\beta J |\mathcal{E}|} \sum_{\sigma} \prod_{(i,j) \in \mathcal{E}} (1 + \mathbb{1}_{\{\sigma_i = \sigma_j\}} (e^{2\beta J} - 1)) \\ &= e^{-\beta J |\mathcal{E}|} \sum_{\mathcal{G}' \subset \mathcal{G}} 2^{\#\{\text{connected components of } \mathcal{G}'\}} (e^{2\beta J} - 1)^{|\mathcal{E}'|}, \end{aligned}$$

where the sum is over all subgraphs $\mathcal{G}' = (\mathcal{V}', \mathcal{E}')$ of the graph $\mathcal{G} = (\mathcal{V}, \mathcal{E})$. The last equality follows by expanding the product into a sum of terms of type $\prod_{(i,j) \in \mathcal{E}'} \mathbb{1}_{\{\sigma_i = \sigma_j\}} (e^{2\beta J} - 1)$, and interpreting the vertices \mathcal{V}' as clusters of agreeing spins in a configuration σ (the spins can be either $+1$ or -1 ; hence the factor 2). In high temperatures, $\beta \ll 1$ and the factor $e^{2\beta J} - 1$ is small (again, the overall global multiplicative factor $e^{-\beta J |\mathcal{E}|}$ can be ignored). The above expression could be regarded as an high temperature expansion of the Ising model (it is slightly different from the usual high temperature expansion that appears in Peierls' argument).

To each configuration \mathcal{G}' , one can associate the dual configuration $(\mathcal{G}')^*$, which contains those edges of the dual graph \mathcal{G}^* which cross edges in the complement $\mathcal{E} \setminus \mathcal{E}'$, and, in addition, isolated vertices which lie inside loops of \mathcal{G}' — see Figure 3.4 for an illustration. In the loop representation, one draws contours between the configuration \mathcal{G}' and the dual configuration $(\mathcal{G}')^*$. The loops form the interfaces associated to the Fortuin-Kasteleyn representation of the Ising model. Imposing boundary conditions, also curves connecting boundary points are obtained. It is important to note that these contours are not the same as the domain walls appearing in the low temperature expansion.

The Fortuin-Kasteleyn representation of the Ising model is often simply called the *FK Ising model*, and the clusters represented by the subgraphs \mathcal{G}' are called *FK clusters*. The interfaces around the clusters in this model have quite different behavior than the domain walls in the Ising model — indeed, at criticality, the latter are described by SLE_3 type curves, whereas the former have been shown (for the case when they touch the boundary) to converge in the scaling limit to self-touching SLE_{κ^*} type curves with $\kappa^* = 16/3$. Similarly as for percolation and self-avoiding walks, there is a duality between the critical Ising and FK Ising models, implemented by the symmetry $\kappa \leftrightarrow 16/\kappa = \kappa^*$, and the outer boundaries of the interfaces of the critical FK Ising clusters look locally like the domain walls in the critical spin Ising model.

3.4. Potts model. Generalizing the Ising model, one can define a spin model with spins having Q possible values. This is called the Q -state Potts model. The energy of a configuration $\sigma: \mathcal{V} \rightarrow \{1, 2, \dots, Q\}$

of spins in the Potts model on the graph $\mathcal{G} = (\mathcal{V}, \mathcal{E})$ is

$$E(\sigma) = -J \sum_{(i,j) \in \mathcal{E}} (\mathbb{1}_{\{\sigma_i = \sigma_j\}} - 1).$$

The Boltzmann weight of a spin configuration is

$$\mathbb{P}[\sigma] = \frac{1}{Z_{\text{Potts}}} \prod_{(i,j) \in \mathcal{E}} e^{\beta J (\mathbb{1}_{\{\sigma_i = \sigma_j\}} - 1)}.$$

To obtain the Fortuin-Kasteleyn representation of the partition function Z_{Potts} , write

$$e^{\beta J (\mathbb{1}_{\{\sigma_i = \sigma_j\}} - 1)} = p \mathbb{1}_{\{\sigma_i = \sigma_j\}} + (1 - p),$$

where $p = 1 - e^{-\beta J}$. The partition function then reads

$$\begin{aligned} Z_{\text{Potts}} &= \sum_{\sigma} \prod_{(i,j) \in \mathcal{E}} e^{\beta J (\mathbb{1}_{\{\sigma_i = \sigma_j\}} - 1)} \\ &= \sum_{\sigma} \prod_{(i,j) \in \mathcal{E}} (p \mathbb{1}_{\{\sigma_i = \sigma_j\}} + (1 - p)) \\ (3.2) \quad &= \sum_{\mathcal{G}' \subset \mathcal{G}} Q^{\#\{\text{connected components of } \mathcal{G}'\}} p^{|\mathcal{E}'|} (1 - p)^{|\mathcal{E}| - |\mathcal{E}'|}. \end{aligned}$$

Note that Equation (3.2) is in fact well-defined for any $Q \geq 0$ and it defines the Fortuin-Kasteleyn representation of the Potts model. A special case with $Q = 2$ gives rise to the FK representation of the Ising model, and the case $Q = 1$ corresponds to a percolation model on edges of the graph (bond percolation). In each FK cluster, one can choose from the Q possible values, and, again, the FK clusters of spins are not the same as the original spins in the Q -state Potts model.

The Potts model has a phase transition in a similar manner as percolation. When $p = 1 - e^{-\beta J}$ is small (high temperature), there is no infinite cluster of aligned spins and the average cluster size is small, whereas for large p (low temperature), there exists a unique infinite cluster of aligned spins. For certain regular lattices, the critical inverse temperature β_c can be determined exactly by duality considerations. For instance, for the planar Q -state Potts model with $Q \geq 2$ on the square lattice, we have $\beta_c = \beta_c(Q) = \frac{1}{J} \log(1 + \sqrt{Q})$, see e.g. [DC11].

In two dimensions, the phase transition is continuous only when $0 \leq Q \leq 4$. In this range, the two-dimensional Potts model is critical and a scale invariant continuum limit exists. At criticality, the interfaces should be again described in the scaling limit by conformally invariant random curves. For the interfaces between the clusters in the FK representation of the Potts model, one expects the scaling limits to be SLE_{κ^*} curves and CLE_{κ^*} loops, where the parameter $\kappa^* \in [4, 8]$ is related to the parameter Q by $Q = 4 \cos^2(4\pi/\kappa^*)$, by arguments using the Hausdorff dimension of the curve, or by CFT considerations [SD87, BB03, RS05, Bef08]. These curves are not simple when $\kappa^* > 4$, as explained in Section 5.5. However, the outer boundaries of the SLE_{κ^*} are again simple curves that look locally like SLE_{κ} curves with $\kappa = 16/\kappa^* \in [2, 4]$. For instance, in the case $Q = 1$, we recover the percolation model with $\kappa^* = 6$ and $\kappa = 8/3$.

In the case of the spin Q -state Potts model, the only values of Q for which a continuous phase transition takes place are $Q = 0, 1, 2, 3, 4$. The interfaces should still correspond with SLE_{κ} and CLE_{κ} processes. The case $Q = 2$ gives the Ising model, with $\kappa = 3$ and $\kappa^* = 16/3$. The limit $Q \rightarrow 0$ should correspond to models known as the loop-erased random walk ($\kappa = 2$) and the uniform spanning tree ($\kappa^* = 8$). Interfaces in the 3- and 4-state spin Potts models are expected (by CFT arguments) to be described by SLE_{κ} , CLE_{κ} processes with $\kappa = 10/3$ and $\kappa = 4$, respectively. Numerical evidence for these values has been found in [WW03, GC07, Cha10].

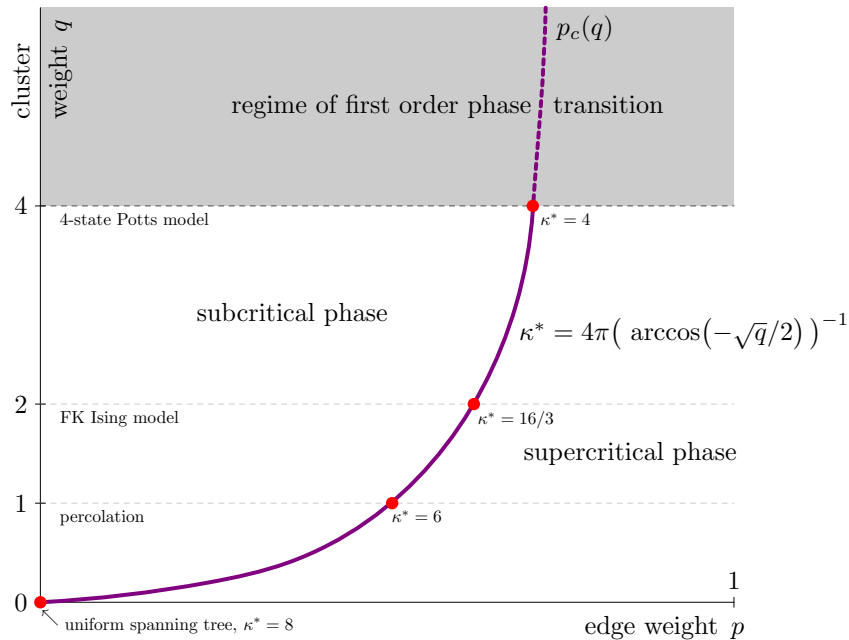


FIGURE 3.5. The phase diagram of the two-dimensional Fortuin-Kasteleyn model. Critical behavior occurs at the critical line $p = p_c(q)$ for $q \in [0, 4]$. At criticality, interfaces in the model should converge to SLE_{κ^*} type curves in the continuum limit. When $q > 4$, there is also a phase transition at $p = p_c(q)$ but it is of first order (discontinuous).

3.5. Fortuin-Kasteleyn model. One can say that the Fortuin-Kasteleyn models provide a unifying family of models for percolation, see e.g. [Gri09, DC11]. The model was introduced by Fortuin and Kasteleyn in 1969. On a finite graph $\mathcal{G} = (\mathcal{V}, \mathcal{E})$, the Fortuin-Kasteleyn model (also known as the random cluster model) is a probability measure on subgraphs $\mathcal{G}' = (\mathcal{V}', \mathcal{E}')$ of \mathcal{G} obtained by assigning weight $q > 0$ for each cluster (i.e., connected component of \mathcal{G}'), weight $p \in [0, 1]$ for each edge in \mathcal{E}' and weight $1 - p$ for each edge in the complement $\mathcal{E} \setminus \mathcal{E}'$:

$$\mathbb{P}[\mathcal{G}'] = \frac{1}{Z_{\text{FK}}} p^{|\mathcal{E}'|} (1 - p)^{|\mathcal{E}| - |\mathcal{E}'|} q^{\#\{\text{connected components of } \mathcal{G}'\}}.$$

The edges of \mathcal{E}' are called open edges, and the complementary edges in $\mathcal{E} \setminus \mathcal{E}'$ are said to be closed.

The cases $q = 1$ and $q = 2$ correspond again with percolation and the FK Ising model, and the case $q = 4$ is equivalent to the 4-state Potts model. When $q \rightarrow 0$, there is only one cluster, and taking the limit in a suitable way ($p \rightarrow 0$ and $\frac{q}{p} \rightarrow 0$ simultaneously), only subgraphs which are spanning trees (connected subgraphs that contain all the vertices and have no loops) of the lattice \mathcal{G} contribute. Each of these is counted with the same weight. This model is called the uniform spanning tree: the tree is chosen uniformly amongst all spanning trees of \mathcal{G} . In fact, the interface between the tree and its dual tree was shown in [LSW04] by Lawler, Schramm, and Werner to converge in the scaling limit to the SLE_8 curve, and a single branch of the tree (which is in fact a loop-erased random walk [Wil96]) to the SLE_2 .

With fixed $q > 0$, the Fortuin-Kasteleyn model should encounter a phase transition at some critical $p_c = p_c(q)$. The behavior should be similar to percolation in the sense that when $p < p_c$, there is no infinite cluster, while for $p > p_c$, there exists a unique infinite cluster. The phase diagram is depicted in Figure 3.5. For different values of q , the phase transition is different. In two dimensions, when $q \in (0, 4]$, the phase transition is expected to be continuous: the infinite-density cluster should converge to zero

when $p \searrow p_c$. On the other hand, when $q > 4$, the phase transition becomes a first order phase transition (discontinuous). In this case, the infinite-density cluster does not converge to zero when $p \searrow p_c$.

When $q \geq 1$, it has been shown [BDC12] that the critical value of p is the number $p_c(q)$ for which the model is self-dual (for the square, hexagonal and triangular lattices), that is, when the configurations \mathcal{G}' and $(\mathcal{G}')^*$ are symmetric (recall again Figure 3.4). In the case of the square lattice (which is a self-dual lattice), the symmetricity requirement implies that $p_c = p_c(q) = \frac{\sqrt{q}}{1+\sqrt{q}}$. This is related to the loop representation of the random cluster model, that is, the loops between the subgraph \mathcal{G}' and its dual $(\mathcal{G}')^*$. Using Euler's formula, one can write the probability measure in terms of the loops as

$$\mathbb{P}[\mathcal{G}'] \propto \left(\frac{p}{(1-p)\sqrt{q}} \right)^{|\mathcal{E}'|} \sqrt{q}^{\#\{\text{loops}\}}.$$

Note that at the self-dual point $p_c = \frac{\sqrt{q}}{1+\sqrt{q}}$, the factor $\frac{p}{(1-p)\sqrt{q}}$ equals one.

As in the case of the Q -state Potts model, the interfaces between the FK clusters \mathcal{G}' and the dual clusters $(\mathcal{G}')^*$ should converge to SLE_{κ^*} curves and CLE_{κ^*} loops with $\kappa^* \in [4, 8]$ and $\sqrt{q} = -2 \cos(4\pi/\kappa^*)$. This has been established rigorously for the cases $q = 0$ (the uniform spanning tree), $q = 1$ (percolation), and $q = 2$ (FK Ising model) — see also Figure 3.5.

3.6. $O(n)$ models. The $O(n)$ models were introduced in order to provide a unifying family for spin models — see e.g. [DC11] for more discussion. After the introduction of the Ising model by Lenz and the (wrong) conjecture by Ising that no phase transition was occurring (but before Peierls' celebrated results in 1936), there was active research in order to find natural generalizations that would exhibit a phase transition. These include the Heisenberg model, where spins are vectors on the sphere \mathbb{S}^2 , and more general spin $O(n)$ models, where the spins lie instead on the sphere \mathbb{S}^{n-1} with $n \geq 4$.

On a finite graph $\mathcal{G} = (\mathcal{V}, \mathcal{E})$, a configuration of the spin $O(n)$ model is an assignment $\sigma: \mathcal{V} \rightarrow \mathbb{S}^{n-1}$ of spins $\sigma_i \in \mathbb{S}^{n-1}$ with probability

$$\mathbb{P}[\sigma] = \frac{1}{Z_{\text{spin } O(n)}} e^{\beta J \sum_{(i,j) \in \mathcal{E}} \sigma_i \cdot \sigma_j},$$

where $\sigma_i \cdot \sigma_j$ denotes the scalar product of the two spins $\sigma_i, \sigma_j \in \mathbb{S}^{n-1}$. When $n = 1$, we obtain the familiar Ising model. The case $n = 2$ is called the XY-model (because of the rotational symmetry), and the case $n = 3$ is the Heisenberg model. For $n = 4$, the $O(4)$ model describes the scalar Higgs sector of the Standard Model. The $O(n)$ model as a lattice field theory is discussed e.g. in the book [Smi02].

The planar $O(n)$ model can be thought of as either a spin model or a model of loops on the plane, in the spirit of the FK models discussed above. In the loop $O(n)$ model, one considers configurations of non-intersecting simple loops on the lattice. For $n = 1$, the loop $O(1)$ -model can be related to the high-temperature expansion of the Ising model. The idea is to approximate the exponential function by

$$e^{x\sigma_i \cdot \sigma_j} \approx 1 + x\sigma_i \cdot \sigma_j \quad \text{where} \quad x = \frac{e^{\beta J} - e^{-\beta J}}{e^{\beta J} + e^{-\beta J}}.$$

Note first that the Ising partition function can be written as

$$Z_{\text{Ising}} = Z_{\text{spin } O(1)} = \sum_{\sigma} \prod_{(i,j) \in \mathcal{E}} e^{\beta J \sigma_i \sigma_j} = \sum_{\sigma} \prod_{(i,j) \in \mathcal{E}} \left(\frac{e^{\beta J} + e^{-\beta J}}{2} + \frac{e^{\beta J} - e^{-\beta J}}{2} \sigma_i \sigma_j \right)$$

On the other hand, with the approximation $e^{x\sigma_i \cdot \sigma_j} \approx 1 + x\sigma_i \cdot \sigma_j$, we have

$$\sum_{\sigma} \prod_{(i,j) \in \mathcal{E}} (1 + x\sigma_i \sigma_j) = \sum_{\sigma} \sum_{\mathcal{E}' \subset \mathcal{E}} \prod_{(i,j) \in \mathcal{E}'} x\sigma_i \sigma_j = \sum_{\mathcal{E}' \subset \mathcal{E}} x^{|\mathcal{E}'|} \sum_{\sigma} \prod_{(i,j) \in \mathcal{E}'} \sigma_i \sigma_j = \sum_{\substack{\text{loop subgraphs} \\ \mathcal{G}' = (\mathcal{V}', \mathcal{E}') \text{ of } \mathcal{G}}} x^{|\mathcal{E}'|},$$

where we noted in the last equality that, due to the symmetry $\sigma_i \leftrightarrow -\sigma_i$, only subgraphs where \mathcal{E}' is a collection of loops contribute — subgraphs $\mathcal{G}' = (\mathcal{V}', \mathcal{E}')$ where at least one vertex has odd degree give zero in the summation over the spin configurations $\sigma \in \{\pm 1\}^{\mathcal{V}'}$.

More generally, for $n \geq 2$, the partition function is an integral over the spins on the sphere

$$(3.3) \quad \int_{(\mathbb{S}^{n-1})^{\mathcal{V}}} \prod_{(i,j) \in \mathcal{E}} (1 + x \sigma_i \cdot \sigma_j) d\sigma = \sum_{\substack{\text{loop subgraphs} \\ \mathcal{G}' = (\mathcal{V}', \mathcal{E}') \text{ of } \mathcal{G}}} n^{\#\{\text{loops in } \mathcal{G}'\}} x^{|\mathcal{E}'|} =: Z_{\text{loop } O(n)}.$$

The graphs \mathcal{G}' that survive the integration over the spin variables $\sigma_i \in \mathbb{S}^{n-1}$ consist of loops on the lattice (with suitable boundary conditions, also paths between boundary points may appear). The number n is also called the loop fugacity. Observe that for $n = 1$, the approximation produces the same partition function as in the original Ising model (up to a universal multiplicative constant): $Z_{\text{Ising}} \propto Z_{\text{loop } O(1)}$.

For integers n , the loop $O(n)$ model can be regarded as an approximation of the high-temperature expansion of the spin $O(n)$ model. However, the model itself makes sense also when n is not an integer (the right hand side of Equation (3.3) defines the partition function).

3.6.1. Phase transitions in planar spin $O(n)$ models. In the planar spin $O(n)$ models with $n \geq 2$, there is a phase transition which is very different from the phase transitions in the Fortuin-Kasteleyn models. For instance, in the case of $n = 2$, in any temperature, the planar $O(2)$ model is disordered. However, there is a critical temperature where a qualitative change of behavior happens. In very high temperatures, the spin correlations of the $O(2)$ model decay exponentially fast in the distance between the spins, whereas in very low temperatures, the decay is only polynomial. It is expected that there is a critical temperature β_c separating these two phases.

This kind of phase transitions are called *Berezinsky-Kosterlitz-Thouless* phase transitions, named after Berezinsky and Kosterlitz-Thouless who studied the spin $O(2)$ model in the 1970s. Compared to the phase transition in the Ising model (that is, the $O(1)$ model), in the phase transition of the $O(2)$ model, there is no ordered phase, no global symmetry is broken (by the Mermin-Wagner theorem), and the order of the phase transition is in fact infinite (i.e., the free energy is infinitely differentiable but not analytic). In the $O(n)$ model with $n \geq 3$, no phase transition is expected, as was already conjectured by Polyakov in 1975, who argued in [Pol75] that the two-dimensional $O(n)$ model with $n \geq 3$ should exhibit exponential decay of correlations at any temperature.

3.6.2. Phase transitions in planar loop $O(n)$ models. Compared to the spin $O(n)$ models, in the loop $O(n)$ models, more critical behavior is expected. Some loop $O(n)$ models should also have a Berezinsky-Kosterlitz-Thouless phase transition between dense and dilute phases. The critical parameter in the loop model case is $x = x_c$, the weight of the length of the loops. When $x < x_c$, the probability of two points i, j to lie on the same loop decays exponentially fast in the distance $|i - j|$, whereas when $x \geq x_c$, this probability has a power law decay. This kind of critical behavior is expected for planar loop $O(n)$ models for $n \in [-2, 2]$, and no phase transition is predicted to occur when $|n| > 2$. The phase diagram of the planar loop $O(n)$ models is depicted in Figure 3.6.

Bernhard Nienhuis [Nie82, Nie84, Nie87, Bax86] argued using so-called Coulomb gas methods that, on the hexagonal lattice, the critical point equals $x_c = x_c(n) = (2 + \sqrt{2 - n})^{-1/2}$. This has been rigorously verified in the case $n = 1$ (the high temperature expansion of the Ising model) using knowledge of the Ising model, see e.g. [DC11]. When $n = 0$, it was proved by Smirnov and Duminil-Copin [DCS12] that indeed $x_c(0) = (2 + \sqrt{2})^{-1/2}$, as Nienhuis predicted. This number is the connective constant of the hexagonal lattice, related to self-avoiding walks.

It is special in the phase transition of the planar loop $O(n)$ models that the model exhibits critical behavior both in the dilute phase at criticality (i.e., when $x = x_c$) and in the dense phase (i.e., when $x > x_c$). Both critical regimes are expected to be conformally invariant in the scaling limit. However, the behavior of the model is different in the two regimes. In the dilute phase, at $x = x_c$, the loops

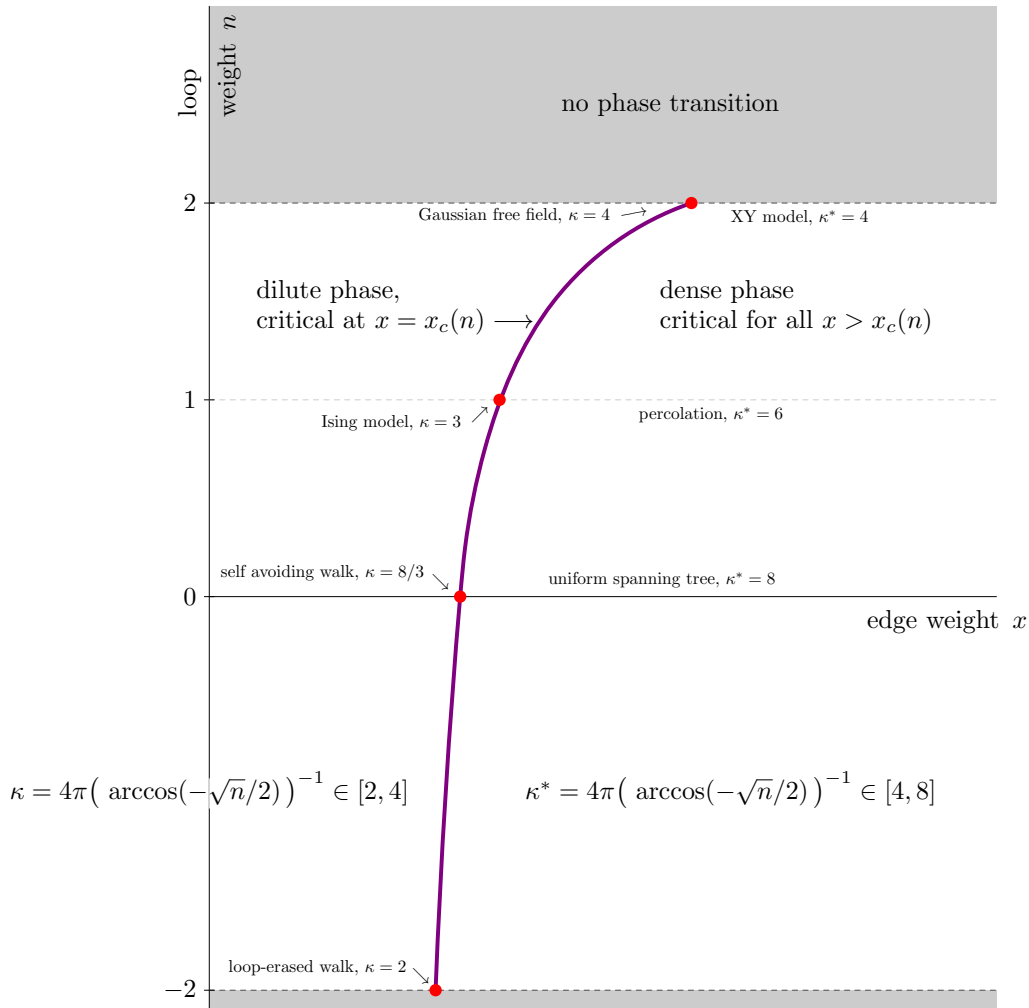


FIGURE 3.6. The phase diagram of the two-dimensional loop $O(n)$ model. The region $x < x_c(n)$ is subcritical: correlations have exponential decay. In the region $x \geq x_c(n)$, correlations behave polynomially and critical behavior is expected. There are two kinds of critical behavior for $n \in [-2, 2]$. First, at the critical line, a continuous Berezinsky-Kosterlitz-Thouless phase transition from the dilute phase ($x < x_c(n)$) to the dense phase ($x > x_c(n)$) takes place. At criticality, interfaces and loops in the dilute model should converge to the conformally invariant SLE_κ and CLE_κ processes with $\kappa \in [2, 4]$. Second, in the dense phase $x > x_c(n)$, due to the polynomial decay of correlations, critical phenomena are also observed. Interfaces and loops in the dense model should converge to SLE_{κ^*} and CLE_{κ^*} , with $\kappa^* \in [4, 8]$.

and interfaces (if boundary conditions are imposed) should converge in the scaling limit to simple CLE_κ loops⁹ and SLE_κ curves with $\kappa \in [2, 4]$ and $n = -2 \cos(4\pi/\kappa)$, whereas in the dense phase, the loops and interfaces should converge to non-simple loops and curves, namely CLE_{κ^*} and SLE_{κ^*} with $\kappa^* \in [4, 8]$ and $n = -2 \cos(4\pi/\kappa^*)$. This is in accordance with the phases of the SLE_κ (and CLE_κ) discussed in Section 5.5: the SLE_κ is a simple curve for $\kappa \leq 4$, self-touching for $\kappa \in (4, 8)$, and space

⁹Strictly speaking, no CLE_κ exists for $\kappa < 8/3$ and $CLE_{8/3}$ is almost surely empty. The SLE_κ curves, however, make sense for all $\kappa \geq 0$.

filling for $\kappa \geq 8$. Note, however, that in general, for $\kappa^* = 16/\kappa$, the values of n are not the same: $-2 \cos(4\pi/\kappa) \neq -2 \cos(4\pi/\kappa^*)$.

We observe that the Fortuin-Kasteleyn model corresponds to $\sqrt{q} = -2 \cos(4\pi/\kappa^*)$ as well. Indeed, the critical FK model with parameters $(p_c(q), q)$, for $q \in [0, 4]$, and the dense loop $O(\sqrt{q})$ model lie in the same universality class and should be described by a similar CFT. However, the two models are not exactly the same — for instance, the energy operators in the two models have different continuum limits.

3.6.3. Relation of the loop $O(n)$ model to other models. In this section, we list some known and predicted results concerning the relationship of the loop $O(n)$ model with other models and the SLE_κ .

- In the special case $n = 0$, no loops are allowed. Then, with suitable boundary conditions, an interface between two boundary points can be added. At the critical point $x = x_c(0)$ (dilute phase), this curve is a *self avoiding random walk* that is conjectured to converge in the scaling limit to the $\text{SLE}_{8/3}$, with central charge $c = 0$. In the dense phase ($x > x_c(0)$), the curve is a uniformly chosen tree containing all vertices of \mathcal{G} , i.e., a *uniform spanning tree*, whose scaling limit is the space filling curve SLE_8 , with central charge $c = -1$ [LSW04].
- The $n = 1$ case corresponds in the dilute phase (at $x = x_c(1)$) to the *Ising model* with $\kappa = 3$ and $c = 1/2$ [Smi01, CN06, Smi10, CDCH⁺14], and in the dense phase ($x > x_c(1)$) to the *percolation model*, with $\kappa^* = 6$ and $c = 0$ [Smi01, Smi10].
- In the case of $n = 2$, the loop $O(2)$ model can be described as a height model, viewing each loop as being oriented in either a clockwise or counterclockwise, such that each loop configuration corresponds to a configuration of integer valued height variables on the dual lattice — see [Car05] for details. These height variables can be thought of as the local height of a crystal surface. This surface is smooth in the low-temperature phase, $x < x_c(2)$, and rough in the high-temperature phase $x > x_c(2)$ (that is, the critical, dense phase). At $x = x_c(2)$, a roughening transition takes place and it is believed that the model corresponds to the *discrete Gaussian free field*¹⁰, dual to the spin $O(2)$ model, and the interfaces correspond to the self-dual value $\kappa = \kappa^* = 4$ with central charge $c = 1$. This model is also equivalent to the *4-state Potts model* ($n = \sqrt{Q}$) and a model called the *double dimer model*, see e.g. [Ken14].
- With $n = -2$, in the dilute phase (at $x = x_c(-2)$), the $O(n)$ model corresponds to the *loop erased random walk* with $\kappa = 2$ and $c = -2$ [LSW04].
- There are no $O(n)$ models corresponding to SLE_κ with $\kappa \in [0, 2)$. For that range, the dual values $\kappa^* > 8$ would give rise to somewhat non-physical space filling and non-reversible curves, see Sections 5.5 and 5.7 for more details.

4. CRITICAL INTERFACES IN STATISTICAL PHYSICS

In Section 3, we saw many examples of critical models described in terms of lattice paths and loops. For instance, in the ferromagnetic Ising model, such interfaces (domain walls) appear between spins which are not aligned, see Figure 3.3. Imposing appropriate boundary conditions, one can force macroscopic random interfaces to appear between given boundary points — even though the starting and end points of these are fixed, the interfaces still have fluctuations inside the domain. For example, in the Ising model, conditioning a segment of the boundary to have spins fixed to a particular state and the complementary segment to have the opposite spins, a macroscopic interface emerges between the boundary points where the boundary conditions change — see Figure 4.1. In the scaling limit, these interfaces converge to SLE_κ curves with $\kappa = 3$, and the loops in the model converge to conformal loop ensembles, CLE_3 [CDCH⁺14].

¹⁰The self-dual value $\kappa = 4$ of the SLE_κ has been shown to correspond to the Gaussian free field (massless free boson) with central charge $c = 1$ [SS05, SS09, SS13]. The SLE_κ curves are the discontinuity curves (level lines) of the free field with Dirichlet boundary conditions. More precisely, the level lines start from boundary points where the Dirichlet boundary conditions jump by a specific amount and this discontinuity of the field propagates inside the domain. In the case of the continuum free field, the mathematical treatment of such level lines (e.g., the almost sure existence of them) is quite subtle since the Gaussian free field is not a function but a distribution in a suitable Sobolev space, see e.g. [She07, MS12]. A relation of the Gaussian free field with domino tilings is described in [Ken00, Ken01].

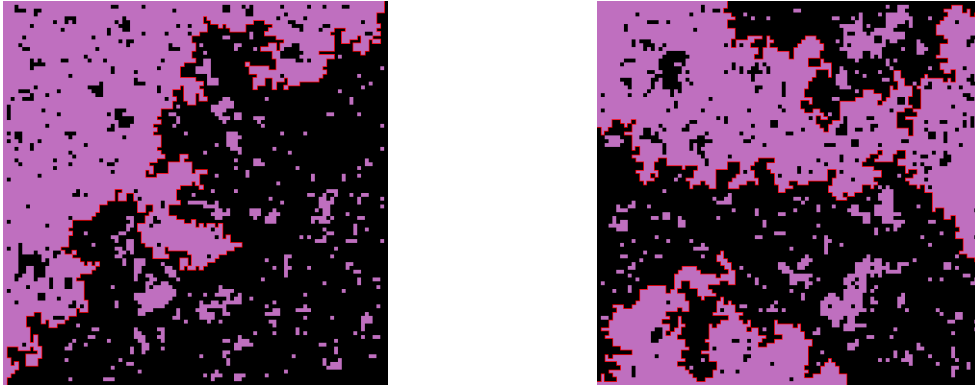


FIGURE 4.1. Simulations of the critical Ising model on a square lattice with alternating boundary conditions (that is, some boundary segments have spins equal to $+1$ and the other segments -1). Interfaces connecting boundary points are highlighted.

4.1. Domain Markov property. The domain Markov property is an important property which holds for many lattice models with local interactions, e.g. for the spin models described in Section 3 (and also for many loop models, with an appropriate definition). It is kind of a memorylessness property of exploration processes (interfaces). Such a property is natural even away from the critical point.

The models described in Section 3 can be defined on graphs \mathcal{G} with arbitrary shape. Because the models have local interactions, the boundary conditions can be naturally defined around a crosscut in the domain, for instance determined by exploring an interface starting from the boundary. The “colors / spins” on both sides of the exploration curve naturally extend the boundary conditions. Consider an exploration process in \mathcal{G} , which e.g. for the Ising model is defined by following the interface between the opposite spins step by step, starting from a point on the boundary where the boundary conditions change, so that on the left one always has negative spins and on the right positive spins, say (see Figure 4.1 for illustrations of such situations). One eventually hits the boundary at another point where the boundary conditions change. Let $\gamma(k)$, for $k = 0, 1, \dots, n$, denote the exploration process in \mathcal{G} , in discrete time. Explore an interface up to some time k_0 . Consider the exploration process $\tilde{\gamma}$ for the model on the smaller grid $\tilde{\mathcal{G}} = \mathcal{G} \setminus \gamma[0, k_0]$, started from the tip $\gamma(k_0)$, where the boundary conditions are taken as before on $\partial\tilde{\mathcal{G}}$ and naturally continued to both sides of the segment $\gamma[0, k_0]$ of $\partial\tilde{\mathcal{G}}$ (in our example, negative on the left of $\gamma[0, k_0]$ and positive on the right). Then (see the proof below), the distribution of the exploration process $\tilde{\gamma}$ associated to the model on the grid $\tilde{\mathcal{G}}$ with the crosscut $\gamma[0, k_0]$ equals the conditional law of the original process γ on the original graph \mathcal{G} given the initial segment $\gamma[0, k_0]$. This is called the *domain Markov property*.

The domain Markov property can be formulated for curves in general, regardless of whether they are in the discrete setting or in continuum. To formalize the property, let $\mathcal{G} \subset \Lambda \subsetneq \mathbb{C}$ a graph on a (simply connected) domain and let $\gamma: [0, 1] \rightarrow \Lambda$ be a (discrete or continuous) curve between two boundary points $\gamma(0) = a \in \partial\Lambda$ and $\gamma(1) = b \in \partial\Lambda$, e.g. the exploration curve above. For simplicity, we assume that the curve is simple, i.e., that it has no self-touchings (more generally, one considers the hull of γ). Suppose the curve is random, with the probability distribution¹¹ $\mathbb{P} = \mathbb{P}^{(\Lambda, a, b)}$. The domain Markov property states that, for any $t \in [0, 1]$ (even more generally, one could let t to be a stopping time), the conditional law of the curve $\gamma[t, 1]$ given its initial segment $\gamma[0, t]$ equals the law $\mathbb{P}^{(\Lambda \setminus \gamma[0, t], \gamma(t), b)}$ associated to the smaller domain $\Lambda \setminus \gamma[0, t]$ with an interface from the tip $\gamma(t)$ to b :

$$(4.1) \quad \mathbb{P}^{(\Lambda, a, b)}[\gamma[t, 1] | \gamma[0, t]] = \mathbb{P}^{(\Lambda \setminus \gamma[0, t], \gamma(t), b)}[\gamma[t, 1]].$$

¹¹One should bear in mind that the probability measure $\mathbb{P}^{(\Lambda; a, b)}$ of γ is in fact defined on a space of curves modulo increasing reparametrizations.

To prove this, let us look at a spin model on the lattice \mathcal{G} with the Boltzmann distribution $\mathbb{P}^{(\Lambda, a, b)}$. We assume that the boundary conditions of the spin model are chosen so that there is an interface between a and b . In this setup, the discrete interface is a set of edges of the dual lattice (as in Figure 3.3) and the probability of an interface configuration γ is the sum of the Boltzmann weights over all possible spin configurations σ compatible with the interface γ . The probability of observing $\gamma = \gamma[0, 1]$ is

$$\mathbf{P}^{(\Lambda, a, b)}[\gamma] = \sum_{\sigma} \mathbf{P}^{(\Lambda, a, b)}[\gamma|\sigma] \mathbb{P}^{(\Lambda, a, b)}[\sigma] = \sum_{\sigma} \mathbf{P}^{(\Lambda, a, b)}[\gamma|\sigma] \frac{e^{-\beta E^{(\Lambda, a, b)}(\sigma)}}{\mathcal{Z}^{(\Lambda, a, b)}},$$

where $\mathbf{P}^{(\Lambda, a, b)}[\gamma|\sigma]$ denotes the conditional probability of the interface $\gamma = \gamma[0, 1]$ given the system in a specific spin configuration σ .

Now, given a segment $\gamma[0, t]$ of the interface, the conditional probability of the rest $\gamma[t, 1]$ of the curve is

$$\mathbf{P}^{(\Lambda, a, b)}[\gamma[t, 1]|\gamma[0, t]] = \frac{\mathbf{P}^{(\Lambda, a, b)}[\gamma[0, t] \cup \gamma[t, 1]]}{\mathbf{P}^{(\Lambda, a, b)}[\gamma[0, t]]} = \frac{\sum_{\sigma} \mathbf{P}^{(\Lambda, a, b)}[\gamma[0, t] \cup \gamma[t, 1]|\sigma] e^{-\beta E^{(\Lambda, a, b)}(\sigma)}}{\sum_{\sigma} \mathbf{P}^{(\Lambda, a, b)}[\gamma[0, t]|\sigma] e^{-\beta E^{(\Lambda, a, b)}(\sigma)}}.$$

Along the crosscut $\gamma[0, t]$, the boundary conditions of the model are obtained by fixing the spins on both sides of the observed interface $\gamma[0, t]$. In terms of the Boltzmann distribution, the weights of the configuration are modified locally along the interface. For instance, for the Ising model, we have

$$e^{-\beta E^{(\Lambda, a, b)}(\sigma)} = \mathcal{Z}^{(\Lambda, a, b)} \mathbb{P}^{(\Lambda, a, b)}[\sigma] = \mathcal{Z}^{(\Lambda \setminus \gamma[0, t], \gamma(t), b)} \mathbb{P}^{(\Lambda \setminus \gamma[0, t], \gamma(t), b)}[\sigma] \prod_{\substack{(i, j) \in \mathcal{E}: \\ (i, j) \perp \gamma[0, t]}} e^{\beta J \sigma_i \sigma_j}.$$

Now the conditional probabilities $\mathbf{P}^{(\Lambda, a, b)}[\gamma[0, t]|\sigma]$ and $\mathbf{P}^{(\Lambda, a, b)}[\gamma[0, t] \cup \gamma[t, 1]|\sigma]$ vanish unless the spins σ_i take different values on both sides of the path $\gamma[0, t]$. This gives restriction to the summation over spins, and the last factors

$$\prod_{\substack{(i, j) \in \mathcal{E}: \\ (i, j) \perp \gamma[0, t]}} e^{\beta J \sigma_i \sigma_j} = \prod_{\substack{(i, j) \in \mathcal{E}: \\ (i, j) \perp \gamma[0, t]}} e^{-\beta J}$$

can be taken out of the summation and they then cancel. We obtain

$$\begin{aligned} \mathbf{P}^{(\Lambda, a, b)}[\gamma[t, 1]|\gamma[0, t]] &= \frac{\sum_{\sigma} \mathbf{P}^{(\Lambda, a, b)}[\gamma[0, t] \cup \gamma[t, 1]|\sigma] \mathbb{P}^{(\Lambda \setminus \gamma[0, t], \gamma(t), b)}[\sigma] \prod_{(i, j) \perp \gamma[0, t]} e^{\beta J \sigma_i \sigma_j}}{\sum_{\sigma} \mathbf{P}^{(\Lambda, a, b)}[\gamma[0, t]|\sigma] \mathbb{P}^{(\Lambda \setminus \gamma[0, t], \gamma(t), b)}[\sigma] \prod_{(i, j) \perp \gamma[0, t]} e^{\beta J \sigma_i \sigma_j}} \\ &= \frac{\prod_{(i, j) \perp \gamma[0, t]} e^{-\beta J} \sum_{\tilde{\sigma}} \mathbf{P}^{(\Lambda, a, b)}[\gamma[0, t] \cup \gamma[t, 1]|\tilde{\sigma}] \mathbb{P}^{(\Lambda \setminus \gamma[0, t], \gamma(t), b)}[\tilde{\sigma}]}{\prod_{(i, j) \perp \gamma[0, t]} e^{-\beta J} \sum_{\tilde{\sigma}} \mathbf{P}^{(\Lambda, a, b)}[\gamma[0, t]|\tilde{\sigma}] \mathbb{P}^{(\Lambda \setminus \gamma[0, t], \gamma(t), b)}[\tilde{\sigma}]} \\ &= \frac{\sum_{\tilde{\sigma}} \mathbf{P}^{(\Lambda, a, b)}[\gamma[0, t] \cup \gamma[t, 1]|\tilde{\sigma}] \mathbb{P}^{(\Lambda \setminus \gamma[0, t], \gamma(t), b)}[\tilde{\sigma}]}{\sum_{\tilde{\sigma}} \mathbf{P}^{(\Lambda, a, b)}[\gamma[0, t]|\tilde{\sigma}] \mathbb{P}^{(\Lambda \setminus \gamma[0, t], \gamma(t), b)}[\tilde{\sigma}]} \end{aligned}$$

where $\tilde{\sigma}: \mathcal{V} \setminus \gamma[0, t] \rightarrow \{\pm 1\}$ are spin configurations on the lattice $\mathcal{G} \setminus \gamma[0, t]$ with the crosscut $\gamma[0, t]$. We can now conclude by observing that the denominator equals one:

$$\sum_{\tilde{\sigma}} \mathbf{P}^{(\Lambda, a, b)}[\gamma[0, t]|\tilde{\sigma}] \mathbb{P}^{(\Lambda \setminus \gamma[0, t], \gamma(t), b)}[\tilde{\sigma}] = \mathbf{P}^{(\Lambda \setminus \gamma[0, t], \gamma(t), b)}[\gamma[0, t]] = 1,$$

and that the numerator thus yields the domain Markov property (4.1) for the law of the segment $\gamma[t, 1]$:

$$\mathbf{P}^{(\Lambda, a, b)}[\gamma[t, 1]|\gamma[0, t]] = \sum_{\tilde{\sigma}} \mathbf{P}^{(\Lambda, a, b)}[\gamma[0, t] \cup \gamma[t, 1]|\tilde{\sigma}] \mathbb{P}^{(\Lambda \setminus \gamma[0, t], \gamma(t), b)}[\tilde{\sigma}] = \mathbf{P}^{(\Lambda \setminus \gamma[0, t], \gamma(t), b)}[\gamma[t, 1]].$$

4.2. Conformal invariance. We formulated the domain Markov property in terms of interfaces γ regardless of whether they lie in the discrete or continuum setup. For scaling limits of discrete interfaces, we expect this memorylessness property to be true even away from the critical point. There is another property, *conformal symmetry*, which is only expected to hold for the scaling limits at criticality. This symmetry can be stated for the interfaces by requiring that the law of the random interface γ is invariant under conformal maps. More generally, the scaling limits of critical models should be described by conformal field theories. Local observables should converge to fields in the CFT and especially, the correlations should converge to CFT correlation functions. We will not pursue the complete description of the scaling limits in this thesis, but concentrate on the properties of interfaces.

Consider measures $\mathbb{P}^{(\Lambda, a, b)}$ on curves in simply connected domains $\Lambda \subsetneq \mathbb{C}$ connecting two given boundary points a and b . Such measures are labeled by the data (Λ, a, b) . Assuming conformal invariance, the measures are determined for any data (Λ', a', b') via

$$(4.2) \quad \mathbb{P}^{(\Lambda, a, b)}[\gamma] = \mathbb{P}^{(\Lambda', a', b')}[\phi \circ \gamma],$$

where $\phi: \Lambda \rightarrow \Lambda'$ is a conformal equivalence such that $\phi(a) = a'$ and $\phi(b) = b'$. By the Riemann mapping theorem (see Section 5.1), such a conformal map ϕ is completely determined by fixing three real parameters, and thus, after fixing the images of the points a and b , one degree of freedom remains. To completely characterize the measures on curves with the data (Λ, a, b) , one has to impose an additional property — the domain Markov property (4.1). This leads to Schramm’s classification of those random curves, i.e., probability measures on the set of curves with the data (Λ, a, b) , that even have a change to arise as scaling limits of critical interfaces. These random curves are known as *Schramm-Loewner evolutions*.

Bibliographical comments. Scale invariance and conformal invariance in relation with statistical physics is most often discussed in the context of conformal field theory. John Cardy has written numerous inspirational and illuminating surveys connecting CFT and statistical mechanics, see e.g. [Car87, Car90, Car96, Car10]. Of course, also in the CFT literature, conformal invariance at criticality is discussed, see e.g. [DFMS97]. Also the recent book [Mus10] is worth mentioning because it gives a modern, unified, and thorough survey on lattice models, critical phenomena as well as QFT and CFT.

5. SCHRAMM-LOEWNER EVOLUTIONS

Around the year 2000, Oded Schramm investigated the implications of the two assumptions of conformal invariance and domain Markov property on the possible probability measures on random curves in continuum domains [Sch00]. He proved that there is an one-parameter family of such random curves, called $(\text{SLE}_\kappa)_{\kappa \geq 0}$, which he called stochastic Loewner evolutions (the terminology has thereafter changed to Schramm-Loewner evolutions to recognize the contributions of Schramm in the theory). The crucial observation of Schramm was that these curves can be described as *growth processes* encoded in conformal mappings called *Loewner chains*. We have seen that, on the lattice, the interfaces may be grown through a discrete exploration process. The Loewner chain is the continuum version of this.

In general, growth processes in two dimensions involve time-dependent subsets of the complex plane \mathbb{C} . These can be curves $\gamma(t)$, or more general domains, e.g., growing families of hulls K_t — a *hull* is a bounded relatively closed subset $K \subset \Lambda$ of a simply connected domain Λ such that also $\Lambda \setminus K$ is simply connected. In Loewner theory, such growth processes are encoded in families of conformal maps, Loewner chains [Loe23]. In this thesis, we will concentrate of growth processes associated to curves, keeping an eye on the growth process description of critical interfaces of planar lattice models.

Bibliographical comments. Surveys related to SLEs and scaling limits include (but are not limited to) the lecture notes and books [KN04, Car05, Law05, BB06, Wer06, Dup06, HKB⁺12, Kem16]. For references concerning growth processes and Loewner theory, we recommend [BB06, Law05, BN16, Kem16], for standard complex analysis, e.g. [Con78, Ahl79, Pom92, Con95], and for stochastic analysis, the reader may consult e.g. [Dur96, RW00a, RW00b, RY05, Dur10].

5.1. Riemann mapping theorem. In Loewner theory, the *Riemann mapping theorem* is the starting point in encoding two-dimensional growth processes in terms of conformal maps. In such a description, one takes a conveniently chosen reference domain (depending on the geometry of the problem, some choices are more convenient than others — the unit disc $\mathbb{D} = \{z \in \mathbb{C} \mid |z| < 1\}$ and the upper half-plane $\mathbb{H} = \{z \in \mathbb{C} \mid \Im(z) > 0\}$ are quite often used). The growth processes in other domains can then be compared with the chosen (hopefully) well-understood reference domain.

The Riemann mapping theorem states that any two simply connected proper subdomains (open, connected subsets) of the complex plane \mathbb{C} are conformally equivalent. Furthermore, fixing three real parameters determines the conformal equivalence between any two such domains uniquely. For us, it is most convenient to fix the images of three boundary points. In this case, the Riemann mapping theorem states that for any two simply connected domains $\Lambda, \Lambda' \subsetneq \mathbb{C}$ and triples $z_1, z_2, z_3 \in \partial\Lambda$ and $w_1, w_2, w_3 \in \partial\Lambda'$ of boundary points¹² appearing in counterclockwise order along the boundary, there exists a unique conformal bijection $\phi: \Lambda \rightarrow \Lambda'$ such that $\phi(z_i) = w_i$, for $i = 1, 2, 3$.

5.2. Loewner evolutions. In its construction as a growth process, the time evolution of the SLE curve γ is encoded in a collection $(g_t)_{t \geq 0}$ of conformal maps $z \mapsto g_t(z)$, called a Loewner chain, satisfying the *Loewner differential equation* [Loe23, Law05, BN16, Kem16]:

$$(5.1) \quad \frac{d}{dt} g_t(z) = \frac{2}{g_t(z) - X_t}, \quad g_0(z) = z,$$

for $z \in \mathbb{H}$ and $t \geq 0$, where X_t is a real-valued function, called the *driving function*. In the general Loewner theory, solutions to the Loewner equation (5.1) give rise to growing families of hulls and the driving function $t \mapsto X_t$ describes the time evolution of a small piece of the growth process.

Note that the solution of (5.1) is defined up to the explosion time $T_z = \inf \{t \geq 0 \mid g_t(z) = X_t\}$, that is, the smallest time when the denominator in the equation is zero. If K_t denotes the closure of the set $\{z \in \mathbb{H} \mid T_z < t\}$, then, for each $t \in [0, T_z)$, the map $z \mapsto g_t(z)$ is the unique conformal isomorphism

$$(5.2) \quad g_t: \mathbb{H} \setminus K_t \rightarrow \mathbb{H} \quad \text{such that} \quad g_t(z) = z + \mathcal{O}\left(\frac{1}{z}\right) \quad \text{as } z \rightarrow \infty.$$

Note that the expansion at infinity fixes three real degrees of freedom: $g_t(\infty) = \infty$, $g_t'(\infty) = 1$, and the constant term in the expansion is zero (this is called the *hydrodynamic normalization*). The inverse map $g_t^{-1}: \mathbb{H} \rightarrow \mathbb{H} \setminus K_t$ grows the hull K_t at each time instant t , and $(K_t)_{t \geq 0}$ is a growth process: $K_s \subset K_t$ for $s < t$. For instance, in the case when $K_t = \gamma(0, t]$ is given by a simple curve γ , we have

$$\gamma(t) = \lim_{\varepsilon \searrow 0} g_t^{-1}(X_t + i\varepsilon).$$

In the simplest case, taking $X_t = 0$, the solution of Equation (5.1) is simply $g_t(z) = \sqrt{z^2 + 4t}$, and the growth process generated by this Loewner evolution is the straight line segment $t \mapsto 2i\sqrt{t}$.

The core observation in the Loewner theory is that also the converse is true: **continuously growing hulls correspond one-to-one to Loewner chains $(g_t)_{t \geq 0}$ with continuous driving functions X_t** . For instance, any curve $\gamma: [0, \infty) \rightarrow \overline{\mathbb{H}}$ can be described in terms of solutions $t \mapsto g_t(z)$ to (5.1) as follows. For simplicity, assume that γ is a simple curve, and let g_t be the conformal maps (5.2) with $K_t = \gamma(0, t]$ for each t . It can be shown that the coefficient of $1/z$ in the expansion of g_t is monotonic increasing in t (it is the capacity of the hull K_t seen from infinity, describing the size of K_t in a conformally invariant way). Therefore, by reparametrizing the time¹³, we may assume that

$$(5.3) \quad g_t(z) = z + \frac{2t}{z} + \mathcal{O}\left(\frac{1}{z^2}\right) \quad \text{as } z \rightarrow \infty.$$

We say that in this case, the time is *parametrized by capacity*.

¹²In this thesis, we will not delve into the details of how boundaries of rough domains should be defined.

¹³Note that the length of the curve is not a useful parametrization if the curve is a fractal, which is the case for instance for the Schramm-Loewner evolution curves. However, one can make sense of a natural parametrization in terms of length by considering “the average time” the curve spends in neighborhoods of points $z \in \mathbb{H}$, see e.g. [LS11, LR15, LV16].

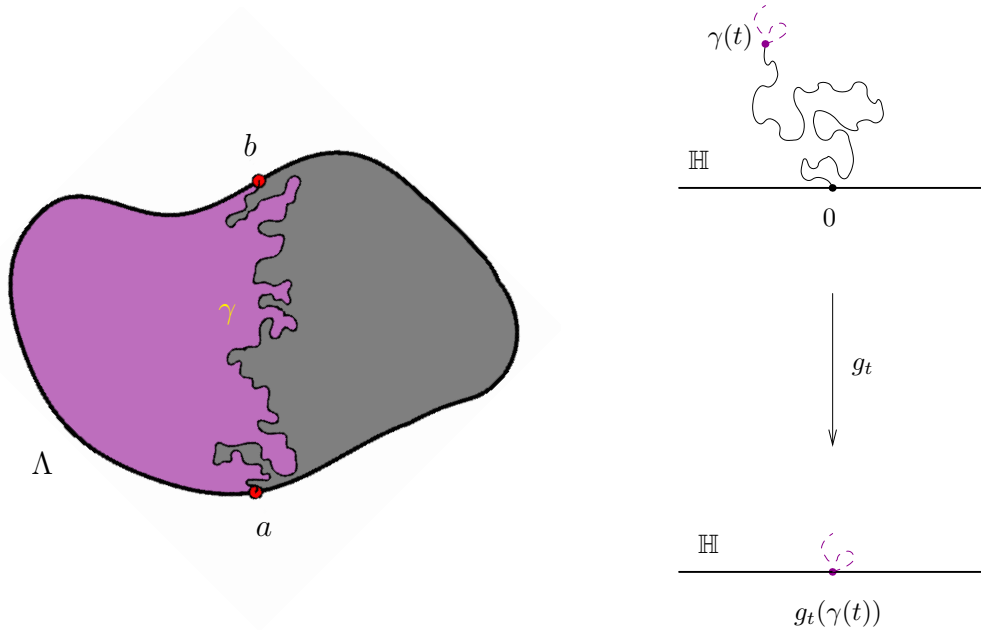


FIGURE 5.1. The left figure depicts a curve γ between two boundary points $a, b \in \partial\Lambda$ of a simply connected domain Λ . The figure on the right illustrates the Loewner map $g_t: \mathbb{H} \setminus K_t \rightarrow \mathbb{H}$. The domain Markov property states that the purple piece of the curve in the lower picture is distributed as the chordal SLE_κ in \mathbb{H} from $g_t(\gamma(t)) = X_t \in \mathbb{R}$ to ∞ . The image of the tip of the SLE_κ curve γ is the driving process $X_t = \sqrt{\kappa}B_t$.

One can show that, for any $t \in [0, \infty)$, the limit

$$X_t := \lim_{\xi \rightarrow \gamma(t) \text{ in } \mathbb{H}} g_t(\xi)$$

exists and it defines a continuous function $t \mapsto X_t$ on $[0, \infty)$. Moreover, for any $z \in \mathbb{H} \setminus K_t$, the process $t \mapsto g_t(z)$ satisfies the Loewner differential equation (5.1) with the driving function X_t . To see this, imagine evolving γ for a short time, from t to $t + \delta t$. Then, the segment $\gamma[t, t + \delta t]$ maps under the map g_t into a short vertical line above the point $X_t \in \mathbb{R}$. Therefore, the map $g_{t+\delta t}$ should look like

$$g_{t+\delta t}(z) \approx X_t + \sqrt{(g_t(z) - X_t)^2 + 4\delta t}.$$

Differentiating this with respect to δt and taking $\delta t \rightarrow 0$ gives Equation (5.1).

More generally, one can define a local growth condition which guarantees that a given growing family $(K_t)_{t \geq 0}$ of hulls is described by a Loewner chain. The requirements are:

- the half-plane capacity of K_t is increasing and continuously differentiable in t
- the mappings (5.2) satisfy the following local growth condition: for any $t \in [0, \infty)$,

$$\bigcap_{\delta > 0} \overline{g_t(K_{t+\delta} \setminus K_t)} = U_t \in \mathbb{R}$$

is a single point and the map $t \mapsto U_t$ is continuous.

If the above conditions hold for $(K_t)_{t \geq 0}$, the mappings g_t satisfy the Loewner differential equation (5.1) (when parametrized as in (5.3)) with the continuous driving function $t \mapsto U_t = X_t$. Such more general growth processes are important for instance when considering curves with self-touchings, such as the chordal SLE_κ with $\kappa > 4$. We refer to the literature for more details [Law05, BN16, Kem16].

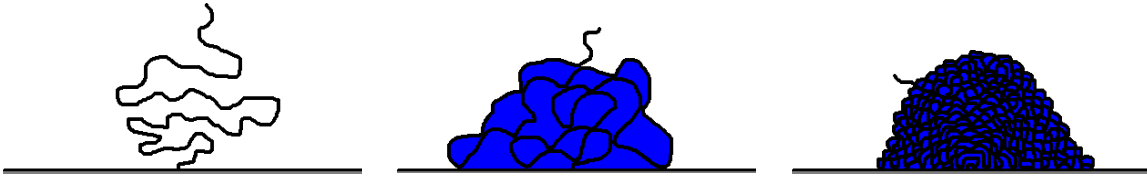


FIGURE 5.2. Illustration of various situations of the behavior of the SLE_κ curve γ . When $\kappa \in [0, 4]$, then γ a simple curve, as depicted in the leftmost figure. When $\kappa \in (4, 8)$, then γ is no longer simple curve, but it bounces off itself and the boundary, as depicted in the middle figure. Finally, for $\kappa \geq 8$, the SLE_κ curve γ winds left and right filling the whole space, as illustrated in the rightmost figure (with κ slightly less than 8). The parameter κ is related to the amount of winding of the curve as it grows (and also to its fractal dimension).

5.3. Schramm-Loewner evolutions. The *chordal Schramm-Loewner evolution* (SLE) is a (probability) measure $\mathbb{P}^{(\Lambda, a, b)}$ on curves indexed by the domain data (Λ, a, b) , where $\Lambda \subsetneq \mathbb{C}$ is a simply connected domain and $a, b \in \partial\Lambda$ are two boundary points of Λ . The (chordal) SLE can then be thought of as a random oriented, non-self-crossing curve in Λ between the two boundary points a, b . It is believed, and in some cases proven¹⁴, to be the scaling limit of chordal interfaces of discrete models in simply connected domains. To describe scaling limits of loops, interfaces in models with more general boundary conditions, or interfaces in non-simply connected domains, variants of the chordal case have been introduced — see e.g. [SW05, She09, MS13, KS15]. These include the radial SLE [Sch00, RS05], dipolar SLE [BBH05], so called $SLE_\kappa(\rho)$ processes [LSW03, SW05], and conformal loop ensembles CLE [She09, SW12], of which the last one is a measure on random collections of loops arising as scaling limits of loops in the models discussed in Section 3. In this thesis, however, we concentrate on the properties of the simplest variant, the chordal SLE_κ .

By conformal invariance of the law $\mathbb{P}^{(\Lambda, a, b)}$ of the chordal SLE_κ curve, it suffices to construct it in our favorite reference domain. We choose to define the SLE_κ in the upper half-plane \mathbb{H} from $a = 0$ to $b = \infty$. According to the Riemann mapping theorem, for any simply connected domain Λ with two boundary points $a, b \in \partial\Lambda$, there exists a conformal bijection $\phi: \Lambda \rightarrow \mathbb{H}$ such that $\phi(a) = 0$ and $\phi(b) = \infty$, and the conformal invariance property gives

$$\mathbb{P}^{(\Lambda, a, b)}[\gamma] = \mathbb{P}^{(\mathbb{H}, 0, \infty)}[\phi \circ \gamma].$$

The SLE_κ curve γ can be constructed as a growth process, where the time evolution is encoded in a solution to the Loewner differential equation (5.1). Originally, Charles Loewner considered in [Loe23] continuous, deterministic driving functions (continuity of X_t ensures that the hulls K_t grow only locally). The groundbreaking idea of Schramm in [Sch00] was to make X_t random: let $X_t = \sqrt{\kappa}B_t$, where B_t is a standard Brownian motion.

One can show that the growth process $(K_t)_{t \geq 0}$ determined by the solution $t \mapsto g_t(z)$ to (5.1) with the random driving function $X_t = \sqrt{\kappa}B_t$ is indeed generated by a random curve $\gamma: [0, \infty) \rightarrow \overline{\mathbb{H}}$ in the sense that $\mathbb{H} \setminus K_t$ is the unbounded component of $\mathbb{H} \setminus \gamma[0, t]$ (we then say that K_t is the hull of γ). By definition, this curve is (a parametrization of) the *chordal SLE_κ curve* in \mathbb{H} from 0 to ∞ (see also Figure 5.1). When the curve is simple, the hull is just the curve itself: $K_t = \gamma(0, t]$, but the curve γ can also bounce off from itself. Then, there are regions enclosed by the curve γ which are not on γ but nevertheless are not reachable from infinity (illustrated in blue in Figure 5.2). We then say that the regions are *swallowed* by the curve γ .

¹⁴The convergence results include the loop-erased random walks and uniform spanning tree [LSW04], interfaces in critical percolation [Smi01, CN07, CN06], the critical Ising and random cluster models [CDCH⁺14], and the discrete Gaussian free field [SS05, SS09, SS13]. However, there are models, such as the self-avoiding walk, for which a conformally invariant scaling limit has not been rigorously proven to exist (conjecturally, the SAW converges to $SLE_{8/3}$).

5.4. Schramm's argument. Suppose that γ is a random curve described by the solutions $t \mapsto g_t(z)$ to the Loewner equation (5.1) with a continuous driving process X_t and assume that X_t is invariant under the reflection¹⁵ $X_t \leftrightarrow -X_t$. Assume also that the law of γ is conformally invariant and that it satisfies the domain Markov property (4.1). Schramm showed that in this situation, we must have $X_t = \sqrt{\kappa}B_t$ for some $\kappa \geq 0$. So Brownian motion is the only possible choice for the driving process in order to describe the scaling limit of a chordal interface in a critical statistical mechanics model (having the reflection invariance) as a Loewner growth process, and the only possible scaling limit is the chordal SLE_κ curve. Relaxing the reflection invariance, however, variants of the SLE_κ can be obtained.

To prove Schramm's result, denote $\hat{\gamma}(s) = g_t(\gamma(t+s)) - X_t$. By the assumed conformal invariance (4.2) and the domain Markov property (4.1), the curve $s \mapsto \hat{\gamma}(s)$ is distributed as γ and it is independent of the realization of $\gamma[0, t]$. The Loewner chain associated to $\hat{\gamma}[0, s]$ is

$$(5.4) \quad \hat{g}_s(z) = g_{t+s} \circ g_t^{-1}(z + X_t) - X_t.$$

Namely, at $z \rightarrow \infty$, we have the following expansions (where the time is parametrized by capacity):

$$g_t(z) = z + \frac{2t}{z} + \mathcal{O}\left(\frac{1}{z^2}\right) \quad \Rightarrow \quad g_t^{-1}(z) = z - \frac{2t}{z} + \mathcal{O}\left(\frac{1}{z^2}\right)$$

so $g_{t+s} \circ g_t^{-1}(z + X_t)$ has the expansion (the ellipses denoting terms of order $\mathcal{O}\left(\frac{1}{z^2}\right)$)

$$\begin{aligned} g_{t+s}(g_t^{-1}(z + X_t)) &= g_{t+s}\left(z + X_t - \frac{2t}{z + X_t}\right) + \dots \\ &= z + X_t - \frac{2t}{z + X_t} + \frac{2(t+s)}{z + X_t} \frac{1}{1 - \frac{2t}{z + X_t}} + \dots \\ &= z + X_t - \frac{2t}{z + X_t} + \frac{2(t+s)}{z + X_t} \left(1 - \frac{2t}{z + X_t} + \dots\right) + \dots \\ &= z + X_t + \frac{2s}{z + X_t} + \dots, \end{aligned}$$

where we expanded $\left(1 - \frac{2t}{z + X_t}\right)^{-1}$ as a geometric series. Subtracting X_t , this is the desired expansion (5.3) for \hat{g}_s . Now, differentiating Equation (5.4) with respect to s , we see that

$$\frac{d}{ds} \hat{g}_s(z) = \frac{2}{\hat{g}_s(z) - (X_{t+s} - X_t)},$$

so the driving process of $\hat{\gamma}$ is $\hat{X}_s = X_{t+s} - X_t$. Moreover, since $s \mapsto \hat{\gamma}(s)$ is distributed as γ and it is independent of $\gamma[0, t]$, the process \hat{X}_s is also independent of $\gamma[0, t]$ and distributed as X_s .

Together with continuity of $t \mapsto X_t$ and the reflection invariance $X_t \leftrightarrow -X_t$, the independence of the increments $X_{t+s} - X_t$ and X_t implies that $X_t = \sqrt{\kappa}B_t + \mu t$, a Brownian motion with drift. Now, the scaling invariance of the law of the curve gives that X_t has to satisfy Brownian scaling: under the transformation $z \mapsto \lambda z$, the driving process transforms as $X_t \mapsto \lambda X_{t/\lambda^2}$, and by conformal invariance, $\lambda X_{t/\lambda^2}$ has the same law as X_t . Therefore, we must have $\mu = 0$. This concludes Schramm's argument.

Moreover, one can show that the converse is also true: each continuously growing family of hulls K_t is realized via the Loewner equation (5.1) and furthermore, for any $X_t = \sqrt{\kappa}B_t$ and $\kappa \geq 0$, the evolution of the hulls in fact is a continuous curve, almost surely [RS05]. The curve cannot have self-crossings because then the driving function $t \mapsto X_t$ would become discontinuous at such points (this gives rise to *branching processes*). However, it can have self-touchings and it can even be a space filling curve. The behavior of the curve is determined by the speed parameter κ , as illustrated in Figure 5.2.

¹⁵The reflection invariance is a very natural assumption which holds for many interfaces discussed in Sections 3 and 4



FIGURE 5.3. Illustration of the SLE_κ curve hitting or swallowing the point x . In either case, the curve hits the real axis. The event is encoded in the Bessel process Y_t being zero: as the curve approaches the real line, the point x becomes less and less visible from infinity, which implies that under the Loewner map g_t , it is mapped very close to X_t .

5.5. Phase transition in κ . The parameter κ characterizes the behavior of the SLE_κ curve: in some sense, it describes the winding speed of the curve in \mathbb{H} . Also, the roughness of the fractal SLE_κ curve is related to κ : the larger κ , the rougher the curve is. There is a drastic change in the behavior of the SLE_κ curve at two specific values of κ . First, when $0 \leq \kappa \leq 4$, the SLE_κ is a simple curve, almost surely. When $\kappa > 4$, the curve almost surely touches itself and the real axis. Finally, when $\kappa \geq 8$, the curve is almost surely space filling.

To see why such a phase transition at $\kappa = 4$ takes place, we need to investigate whether the SLE_κ curve hits itself (or the real axis). To study the behavior of the curve, we consider the time evolution of the tip of the curve with respect to a chosen reference point $x \in \mathbb{R}$. Let

$$Y_t = Y_t(x) = \frac{1}{\sqrt{\kappa}} (g_t(x) - X_t) = \frac{g_t(x)}{\sqrt{\kappa}} - B_t.$$

The process $Y_t = Y_t(x)$ encodes the times when the SLE_κ curve hits or swallows the point x : at times when Y_t is zero, the curve either hits or swallows x (see Figure 5.3). In either case, it then also has to hit the real axis. Using the Loewner equation (5.1), one can calculate the stochastic differential

$$dY_t = \frac{2/\kappa}{Y_t} dt + dB_t.$$

This means that Y_t is a *Bessel process* of effective dimension $1 + 4/\kappa$. For such a process it is known that when $\kappa \leq 4$, the process Y_t never hits zero, whereas for $\kappa > 4$, the process Y_t hits zero in finite time, almost surely. Recall that in terms of the behavior of the SLE_κ curve, Y_t hitting zero means that the curve hits or swallows the point $x \in \mathbb{R}$. Thus, when $\kappa \leq 4$, the curve never hits the real axis, almost surely, and by a similar argument, it never hits itself (i.e., it is a simple curve). On the other hand, when $\kappa > 4$, the curve hits both itself and the real axis almost surely. A more rigorous treatment of the phase transition at $\kappa = 4$ (and at $\kappa = 8$) can be found e.g. in [Law05, BN16, Kem16].

The phase transition at $\kappa = 8$, when the curve becomes space filling, can be proved by a more careful analysis of the process Y_t . One has to keep track of the swallowing of two points $x, y \in \mathbb{R}$ simultaneously, and also to consider $Y_t = Y_t(z)$ for a point $z \in \mathbb{H}$ in the interior of the upper half-plane. We refer to the literature for the detailed arguments, e.g. [Law05, BN16, Kem16]. Note that the property that SLE_κ is space filling for $\kappa \geq 8$ is also visible in the behavior of the Hausdorff dimension of the curve: the dimension is $\kappa/8 + 1$ when $0 \leq \kappa \leq 8$, and 2 when $\kappa \geq 8$.

5.6. $\kappa \leftrightarrow 16/\kappa$ duality. When $\kappa > 4$, the SLE_κ curve touches itself from time to time, and as a result, regions of \mathbb{H} are swallowed by the curve, as illustrated in Figure 5.2. However, one can also trace the frontier of the hull of the SLE_κ curve, that is, its outer boundary. The frontier is a simple curve which in fact locally looks like an SLE_{κ^*} with $\kappa^* = 16/\kappa$ [Dup00, Bef04, Dup04, Dub07, Zha08a]. In the language of conformal field theory, the two SLEs correspond with CFTs with the same central charge $c(\kappa) = \frac{1}{2\kappa}(\kappa - 6)(8 - 3\kappa) = c(\kappa^*)$. It is to be noted, however, that the correspondence is only local — in

fact, the frontier is a non-trivial variant of the chordal SLE_{κ^*} where the driving function is of the form $\sqrt{\kappa^*}B_t + \mu t$ with a non-zero (and rather complicated) drift function μ .

5.7. Reversibility. The definition of the chordal SLE_{κ} curve is a priori very asymmetric: the starting and end points are specified, but the Loewner chain grows an oriented curve from the starting point to the endpoint. However, interfaces in discrete models apparently do not care about the orientation. Therefore, the SLE_{κ} curves should also be reversible with respect to switching the starting and end points. This is not clear at all from the definition, since in \mathbb{H} the mapping $z \mapsto 1/z$ interchanging 0 and ∞ also changes the parametrization of the curve drastically. This can be dealt with [Zha08b] but the rigorous proof is very involved.

It turns out that the chordal SLE_{κ} curve is reversible only in the regime $\kappa \in [0, 8]$. This might be related to the fact that there are no $O(n)$ models corresponding to SLE_{κ} with $\kappa \in [0, 2)$, as in this regime, the dual value would be $\kappa^* = 16/\kappa > 8$. The limiting case $\kappa^* = 8$ corresponds to the uniform spanning tree, which is the dense phase of the $O(0)$ model. The dual value $\kappa = 2$, the loop erased random walk, appears as the critical dilute phase of the $O(-2)$ model, see also Figure 3.6.

5.8. Cardy’s formula for crossing probabilities. One of the remarkable successes of the conformal field theory description of critical models of statistical mechanics is John Cardy’s prediction of crossing probabilities in critical percolation [Car92], that is, the probability that there exists a yellow cluster connecting to opposite sides of a rectangle¹⁶. Cardy’s original derivation of the crossing formula relied on arguments from boundary CFTs and the formula was conjectured to be conformally invariant. Numerical evidence supporting the prediction was obtained in [LPSA94]. This percolation crossing formula has now been rigorously proved by Smirnov [Smi01] — it was in fact a crucial ingredient in the proof of the conformal invariance of critical percolation in the scaling limit, an achievement worth the prestigious Fields medal.

In the continuum, Cardy’s formula applies to SLE_6 , the scaling limit of critical percolation interfaces (as Smirnov proved in his celebrated work). It may in fact be extended to a formula valid for arbitrary $\kappa > 4$, see [LSW01b, LSW01c, LSW02c] and in arbitrary simply connected domains. We give below the more general crossing formula.

Consider the event that in the percolation configuration, there is a yellow cluster connecting two disjoint boundary segments AB and CD . In the SLE framework, this crossing problem can be converted into calculating the probability of the event that the SLE_6 curve hits a suitable interval. By conformal invariance, we may consider the problem in the upper half-plane \mathbb{H} with the segments $AB = (-\infty, x_1)$ and $CD = (0, x_2)$, where $x_1 < 0$ and $x_2 > 0$, (see Figure 5.4). In the lattice picture, one would then consider critical percolation on an infinite lattice in the upper half-plane, the boundary conditions chosen such that the segments $(-\infty, 0)$ and $(0, +\infty)$ would be colored purple and yellow, respectively. Then, an exploration process could be defined starting from the origin and following the interface between the two colors. In the continuum limit, this interface would then be the chordal SLE_6 curve.

Now, because $\kappa = 6 > 4$, the curve hits the boundary $\partial\mathbb{H} = \mathbb{R}$, so every point $x \in \mathbb{R}$ is eventually swallowed by the SLE_6 curve. In particular, either the point x_1 is swallowed before x_2 or vice versa. These two cases correspond to the event of having a yellow cluster connecting $AB = (-\infty, x_1)$ and $CD = (0, x_2)$, and the complementary event, as illustrated in Figure 5.4. In particular, there is such a yellow cluster if and only if x_1 is swallowed before x_2 . In fact, this argument works for any $\kappa > 4$ (this is the regime when the SLE_{κ} swallows points). The crossing probability can thus be written in the form

$$\mathbb{P}[\text{there exists a yellow crossing } (-\infty, x_1) \rightarrow (0, x_2)] = \mathbb{P}[x_1 \text{ is swallowed before } x_2] =: P(x_1, x_2).$$

¹⁶Cardy’s crossing probability is not the only formula predicted for critical percolation using CFT arguments. For instance, Watts predicted another crossing formula for percolation in [Wat96], see [Dub06] for the rigorous proof. Watts’ formula gives the probability in a rectangle of the existence of yellow clusters crossing simultaneously from the right to left and from top to bottom. There is also a formula proved by Schramm [Sch01] for the probability that a given bulk point lies to the left of the exploration curve.

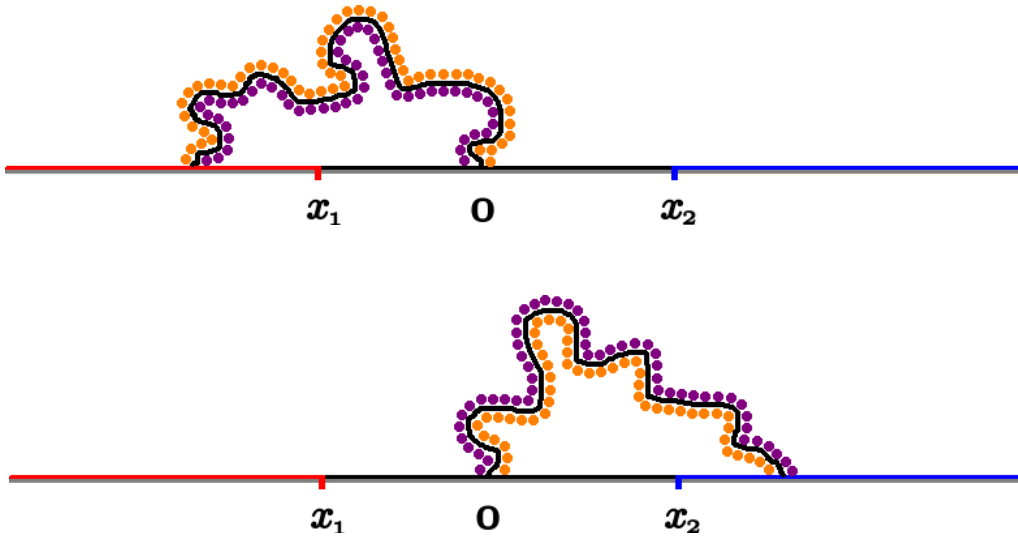


FIGURE 5.4. Illustration of the crossing event from $(-\infty, x_1)$ to $(0, x_2)$ by yellow hexagons in critical percolation, and how it is related to the SLE_6 curve swallowing the point x_1 before the point x_2 . In the top figure, such a crossing event happens and the exploration process swallows x_1 before x_2 , whereas in the bottom figure, the point x_2 is swallowed before x_1 and the purple crossing forms an obstruction against having a yellow crossing from $(-\infty, x_1)$ to $(0, x_2)$.

By the domain Markov property of the SLE_κ (for any $\kappa > 4$), conditioning on an initial segment $\gamma[0, t]$ of the SLE_κ curve, we get a (local) martingale:

$$\begin{aligned} M_t &= \mathbb{P}[x_1 \text{ is swallowed before } x_2 \mid \gamma[0, t]] \\ &= \mathbb{P}[g_t(x_1) - X_t \text{ is swallowed before } g_t(x_2) - X_t] \\ &= P(g_t(x_1) - X_t, g_t(x_2) - X_t), \end{aligned}$$

because the domain Markov property for the SLE_κ says that conditioning on $\gamma[0, t]$ amounts to mapping by the Loewner map $g_t - X_t$ and starting over. Let us calculate the stochastic differential of this martingale. First, using the Loewner equation (5.1) and the equalities $X_t = \sqrt{\kappa}B_t$ and $d\langle B, B \rangle_t = dt$, one can calculate that

$$d(g_t(x) - X_t) = \frac{2 dt}{g_t(x) - X_t} - \sqrt{\kappa} dB_t, \quad d\langle g_t(x) - X_t, g_t(y) - X_t \rangle_t = \kappa dt.$$

Itô's formula then gives

$$\begin{aligned} dM_t &= dP(g_t(x_1) - X_t, g_t(x_2) - X_t) \\ &= dt \left(\frac{\kappa}{2} \left(\frac{\partial}{\partial x_1} + \frac{\partial}{\partial x_2} \right)^2 + \frac{2}{g_t(x_1) - X_t} \frac{\partial}{\partial x_1} + \frac{2}{g_t(x_2) - X_t} \frac{\partial}{\partial x_2} \right) P(g_t(x_1) - X_t, g_t(x_2) - X_t) \\ &\quad - \sqrt{\kappa} dB_t \left(\frac{\partial}{\partial x_1} + \frac{\partial}{\partial x_2} \right) P(g_t(x_1) - X_t, g_t(x_2) - X_t) \end{aligned}$$

Equating the drift term of the martingale M_t with zero, one arrives at an ordinary differential equation¹⁷ for the crossing probability:

$$\left(\frac{\kappa}{2} \left(\frac{\partial}{\partial x_1} + \frac{\partial}{\partial x_2} \right)^2 + \frac{2}{x_1} \frac{\partial}{\partial x_1} + \frac{2}{x_2} \frac{\partial}{\partial x_2} \right) P(x_1, x_2) = 0.$$

By investigating the behavior of the SLE_κ curve, one can deduce the appropriate boundary conditions for the solution $P(x_1, x_2)$. Clearly, when one of the points is zero, it will be swallowed first. Hence,

$$P(0, x_2) = 1, \quad P(x_1, 0) = 0.$$

Applying a scaling, the solution to this problem reduces to an expression involving the ratio $\eta = -\frac{x_1}{x_2} > 0$ and the hypergeometric function ${}_2F_1$,

$$P(x_1, x_2) = \frac{\Gamma\left(\frac{2}{\kappa}(\kappa - 4)\right)}{\Gamma\left(\frac{1}{\kappa}(\kappa - 4)\right)^2} \int_\eta^\infty u^{-\frac{4}{\kappa}} (1+u)^{\frac{2}{\kappa}(4-\kappa)} du = 1 - \frac{\kappa}{\kappa - 4} \eta^{1-4/\kappa} {}_2F_1\left(\frac{4}{\kappa}, 1 - \frac{4}{\kappa}, 2 - \frac{4}{\kappa}; \frac{\eta}{\eta + 1}\right).$$

Taking $\kappa = 6$, this reduces to Cardy's formula for percolation crossings [Car92].

The above arguments were purely probabilistic. In this thesis, we omit the (quite nice!) CFT derivation of the crossing formula but strongly encourage the reader to take a look at the CFT point of view in the literature, e.g. [BB06].

As a final remark, we note that Cardy's crossing formula has a particularly simple form in a equilateral triangle. Let $A = e^{i\pi/3}$, $B = 1$, and $C = 0$ be the corners of the triangle Δ . In the scaling limit, the probability of the crossing event from AB to $CD = [0, x]$ is a linear function:

$$\mathbb{P}[\text{there is a crossing from } [e^{i\pi/3}, 1] \text{ to } [0, x]] \longrightarrow x \quad \text{in the continuum limit.}$$

In fact, Cardy's formula (with $\kappa = 6$) is related to the Schwarz-Christoffel transformation from $(\mathbb{H}, 0, 1, \infty)$ to $(\Delta, 0, 1, e^{i\pi/3})$, see e.g. [BN16] for details.

6. RESTRICTION PROPERTIES OF SLE_κ

In general, one might be interested in what happens to the measure of a random curve in a domain Λ when perturbing Λ . For instance, if $\Lambda' \subset \Lambda$, how are the measures in Λ and Λ' related? Can the measure of random curves in Λ' be regarded as a restriction of the measure of random curves in the whole domain Λ ? Also, what happens in perturbation of the boundary conditions? In this thesis, we are of course interested in the case of the SLE_κ curves, and such questions arise naturally in discrete lattice models of statistical mechanics, whose scaling limits involve SLEs.

More formally, suppose $\Lambda' \subset \Lambda$ (assume both Λ and Λ' are simply connected) and let $a, b \in \partial\Lambda \cap \partial\Lambda'$. One might hope that the measure $\mathbb{P}^{(\Lambda, a, b)}$ of random curves from a to b in Λ would be the same as the measure $\mathbb{P}^{(\Lambda', a, b)}$ of random curves in the smaller domain from a to b . This might be achieved by conditioning the curve $\gamma \sim \mathbb{P}^{(\Lambda, a, b)}$ to stay in Λ' . Note, however, that when $\kappa > 4$, the SLE_κ curves have self-touchings and they also bounce off the boundary of the domain. Therefore, conditioning such an SLE_κ curve to stay in a smaller subdomain does not really make sense, since this would require conditioning on an event of probability zero — indeed, for the chordal SLE_κ curve γ in (Λ, a, b) with $\kappa > 4$, we have $\mathbb{P}[\gamma \subset \Lambda'] = 0$ almost surely. On the other hand, when $0 \leq \kappa \leq 4$, we have $\mathbb{P}[\gamma \subset \Lambda'] > 0$ almost surely, so the conditioning makes sense. In the latter case, one can look at so called restriction measures and show that the above type of property indeed holds for $\text{SLE}_{8/3}$ (and for $\kappa = 8/3$ only) — see Section 6.2 for details.

¹⁷In fact, this differential equation is the null-state equation for the primary field $\Psi_{1,2}$ (or $\Psi_{2,1}$) of Kac conformal weight $h_{1,2} = \frac{6-\kappa}{2\kappa}$ (or $h_{2,1}$) in a degenerate boundary CFT with central charge $c(\kappa) = \frac{1}{2\kappa}(\kappa - 6)(8 - 3\kappa)$ [BPZ84b, Car84, Car86, DFMS97, Car06]. The reason for this is that starting points x of chordal SLE_κ curves correspond with boundary changing operators $\Psi_{1,2}(x)$ and $\Psi_{2,1}(x)$ having degeneracy at level two [BB02, BB03, FW03].

But what to do with self- and boundary touching curves? Instead of the difficult task of conditioning the curve to stay in a smaller domain, one can look at an initial segment of the curve before it exits Λ' . This leads to the concept of *locality*.

6.1. Locality of SLE_6 . In the discrete setup, the idea of the locality property is that the growth process does not feel the boundary of the domain as long as it does not hit it. For an example, consider interfaces in critical percolation. Take two copies of the same sample on \mathcal{G} and add boundary conditions in such a way that in one sample, yellow hexagons are added to a boundary segment between a and b and purple hexagons to the complementary boundary segment, and in the other sample, do the same with the point b replaced by c . Then, the percolation configurations agree inside the domain but on the boundary segment bc between b and c not containing a , the colors disagree. Start now exploring the interface from a . By the locality property of percolation (which is a consequence of the independence of the colorings of the hexagons), the exploration processes in (\mathcal{G}, a, b) and (\mathcal{G}, a, c) agree until the first time of hitting the boundary segment bc .

The notion of locality can also be formulated in continuum, and in fact, the only possible value of κ that can be related to the scaling limit of the percolation interfaces can be identified — it turns out that there is exactly one value of κ for which the locality property holds: $\kappa = 6$. This was first proved in [LSW01b]. Later, a much simpler proof appeared in [LSW03]. Locality allowed to strengthen the conjecture that SLE_6 was the scaling limit of critical percolation interfaces even before the rigorous proof of Smirnov.

The locality property can be studied by comparing two SLE_κ processes in \mathbb{H} , one from 0 to ∞ and one from 0 to $x \in \mathbb{R}$. Let γ be the SLE_κ in $(\mathbb{H}, 0, \infty)$. Let $\phi: \mathbb{H} \rightarrow \mathbb{H}$ be a conformal map with $\phi(0) = 0$ and $\phi(\infty) = x$. Then, by conformal invariance, the image curve $\tilde{\gamma} = \phi \circ \gamma$ is an SLE_κ in $(\mathbb{H}, 0, x)$. Let K_t be the hull of γ and let $g_t: \mathbb{H} \setminus K_t \rightarrow \mathbb{H}$ be the Loewner chain associated to γ satisfying the Loewner equation (5.1). Let also \tilde{K}_t be the hull of $\tilde{\gamma}$ and let $\tilde{g}_t: \mathbb{H} \setminus \tilde{K}_t \rightarrow \mathbb{H}$ be the Loewner chain associated to $\tilde{\gamma}$, normalized as in (5.2) (that is, in hydrodynamic normalization). Then, \tilde{g}_t satisfies a slightly modified Loewner equation:

$$(6.1) \quad \frac{d}{dt} \tilde{g}_t(z) = \frac{2a_t}{\tilde{g}_t(z) - \tilde{X}_t},$$

where the time parametrization is not at our disposal — hence the factor a_t in the equation. Finally, denote by $\phi_t = \tilde{g}_t \circ \phi \circ g_t^{-1}: \mathbb{H} \rightarrow \mathbb{H}$. Then, the driving process of the curve $\tilde{\gamma}$ is $\tilde{X}_t = \phi_t(X_t)$, where $X_t = g_t(\gamma(t)) = \sqrt{\kappa}B_t$ is the driving process of the chordal SLE_κ curve γ .

Differentiating the equation $\tilde{g}_t \circ \phi = \phi_t \circ g_t$ with respect to t and replacing $g_t(z) = w$, we get

$$(6.2) \quad \frac{2a_t}{\phi_t(w) - \tilde{X}_t} = \frac{d}{dt} \phi_t(w) + \phi_t'(w) \frac{2}{w - X_t}.$$

Because $\phi_t(w)$ is non-singular at $w = X_t$, we see that

$$\frac{2a_t}{\phi_t(w) - \tilde{X}_t} = \phi_t'(X_t) \frac{2}{w - X_t} + \mathcal{O}(1) \quad \text{as } w \rightarrow X_t.$$

Since $\tilde{X}_t = \phi_t(X_t)$, we get $a_t = (\phi_t'(X_t))^2$. Expanding further in powers of $w - X_t$, the right hand side of Equation (6.2) becomes

$$\begin{aligned} & \frac{d}{dt} \phi_t(X_t) + \frac{2}{w - X_t} (\phi_t'(X_t) + (w - X_t)\phi_t''(X_t)) + \mathcal{O}(w - X_t) \\ &= \frac{d}{dt} \phi_t(X_t) + \phi_t'(X_t) \frac{2}{w - X_t} + 2\phi_t''(X_t) + \mathcal{O}(w - X_t) \quad \text{as } w \rightarrow X_t, \end{aligned}$$

and the left hand side of Equation (6.2) becomes

$$\begin{aligned}
\frac{2a_t}{\phi_t(w) - \phi_t(X_t)} &= \frac{2a_t}{(w - X_t)\phi'_t(X_t) + \frac{1}{2}(w - X_t)^2\phi''_t(X_t)} + \mathcal{O}(w - X_t) \\
&= \frac{2a_t}{(w - X_t)\phi'_t(X_t)} \left(\frac{1}{1 + (w - X_t)\frac{\phi''_t(X_t)}{2\phi'_t(X_t)}} \right) + \mathcal{O}(w - X_t) \\
&= \frac{2a_t}{(w - X_t)\phi'_t(X_t)} \left(1 - (w - X_t)\frac{\phi''_t(X_t)}{2\phi'_t(X_t)} \right) + \mathcal{O}(w - X_t) \\
&= \frac{2(\phi'_t(X_t))^2}{(w - X_t)\phi'_t(X_t)} - 2a_t \frac{\phi''_t(X_t)}{2(\phi'_t(X_t))^2} + \mathcal{O}(w - X_t) \\
&= \phi'_t(X_t) \frac{2}{(w - X_t)} - \phi''_t(X_t) + \mathcal{O}(w - X_t) \quad \text{as } w \rightarrow X_t,
\end{aligned}$$

where we used the equality $a_t = (\phi'_t(X_t))^2$ and the expansion of a geometric series. Combining, we find

$$\frac{d}{dt} \phi_t(X_t) = -3\phi''_t(X_t).$$

Now, applying Itô's formula to the driving process $\tilde{X}_t = \phi_t(X_t)$, we get

$$d\tilde{X}_t = d(\phi_t(X_t)) = (d\phi_t)(X_t) + \phi'_t(X_t)dX_t + \frac{\kappa}{2}\phi''_t(X_t)dt = \phi'_t(X_t)dX_t + \left(\frac{\kappa}{2} - 3\right)\phi''_t(X_t)dt.$$

Next we make a time change $t \mapsto s(t)$ as follows. Set $\hat{X}_{s(t)} := \tilde{X}_t = \phi_t(X_t)$ and $s(t) := \int_0^t (\phi'_u(X_u))^2 du$. The, by general Itô theory, because $X_t = \sqrt{\kappa}B_t$, the process $W_s = W_{s(t)} = \frac{1}{\sqrt{\kappa}} \int_0^t \phi'_u(X_u)dX_u$ is a Brownian motion and we have

$$d\hat{X}_s = \sqrt{\kappa}W_s + \left(\frac{\kappa}{2} - 3\right) \frac{\phi''_{t(s)}(X_{t(s)})}{(\phi'_{t(s)}(X_{t(s)}))^2} ds.$$

This time change is exactly what we need to parametrize the time by dt instead of $a_t dt = (\phi'_t(X_t))^2 dt$ in Equation (6.1). We thus find that the function $\hat{g}_s(t) := \tilde{g}_t$ satisfies the Loewner equation (5.1) with the time parametrized by capacity:

$$\frac{d}{ds} \hat{g}_s(w) = \frac{2}{\hat{g}_s(w) - \hat{X}_s}.$$

Therefore, the curves γ and $\tilde{\gamma}$ are identically distributed if and only if the drift term in $d\hat{X}_s$ is zero, that is, when $\kappa = 6$.

In fact, one can prove that

$$\frac{\phi''_{t(s)}(X_{t(s)})}{(\phi'_{t(s)}(X_{t(s)}))^2} = \frac{2}{\tilde{X}_t - \tilde{g}_t(x)},$$

so defining $\hat{Y}_s := \hat{g}_s(x)$ we can simplify the above SDEs to the form

$$d\hat{X}_s = \sqrt{\kappa}W_s + \frac{\kappa - 6}{\hat{X}_s - \hat{Y}_s} ds, \quad d\hat{Y}_s = \frac{2}{\hat{Y}_s - \hat{X}_s} ds.$$

This kind of a pair of SDEs defines what is known as the $\text{SLE}_\kappa(\rho)$ process, with $\rho = \kappa - 6$ in this case. This process feels an additional marked point (a force point) on the boundary, which evolves according to the driving process \hat{Y}_s . The effect of the force point is visible in the drift term of the driving process \hat{X}_s of the $\text{SLE}_\kappa(\rho)$ curve. We see that when $\kappa = 6$, the force point does not affect the $\text{SLE}_\kappa(0)$ curve at all — this is evidence of locality!

Similar calculations as above also give a more general locality property for the SLE_6 . This property can be formulated as follows. Let $\Lambda' \subset \Lambda$ such that both Λ and Λ' are simply connected and let $a \in \partial\Lambda$

be a point such that Λ' is a neighborhood of a . Let also $b \in \partial\Lambda$ and $b' \in \partial\Lambda'$. Let $\gamma \sim \mathbb{P}^{(\Lambda, a, b)}$ and $\gamma' \sim \mathbb{P}^{(\Lambda', a, b')}$ be two SLE_κ curves. Then, for any simply connected neighborhood $N \ni a$ of the starting point a of both curves in Λ' such that the end points of the curves are away from N (that is, $b, b' \notin \overline{N}$), the curves γ and γ' stopped before either of them exits N have the same law if and only if $\kappa = 6$.

6.2. Restriction property of $\text{SLE}_{8/3}$. Let us then turn to the property known as *conformal restriction*. In this case, we perturb the domain Λ and condition the curve to stay in the smaller domain $\Lambda' \subset \Lambda$ (instead of stopping it) — this can be done for the SLE_κ when $\kappa \leq 4$. The idea of invariance under domain perturbation is more general: one can define so called *restriction measures* on conformally invariant random hulls. It turns out that the only case when such a measure is supported on a simple curve is the case of $\text{SLE}_{8/3}$. Furthermore, there is a one-parameter family of restriction measures, conventionally parametrized by α . These measures can be characterized in terms of the SLE_κ and Brownian loops, as described briefly in Section 6.3 below.

Consider the SLE_κ curve γ in $(\mathbb{H}, 0, \infty)$. Let $A \subset \mathbb{H}$ be a hull. Suppose A is at some finite distance from 0 and ∞ . Let $\phi_A: \mathbb{H} \setminus A \rightarrow \mathbb{H}$ be a conformal map removing A , normalized by $\phi_A(0) = 0$ and $\phi_A(\infty) = \infty$. Conditioning γ not to hit A , we can consider the curve $t \mapsto (\phi_A \circ \gamma)(t)$. The *restriction property* states that, conditionally on the event $\{\gamma \cap A = \emptyset\}$, the curve $\phi_A \circ \gamma$ is distributed as the chordal SLE_κ in $\mathbb{H} \setminus A$ from 0 to ∞ (up to a time change).

One can prove that $\kappa = 8/3$ is the only value of κ for which the restriction property holds for the SLE_κ . The argument goes as follows. One first shows that the restriction property holds if and only if ($\kappa < 4$ and) the probability that γ hits A is of the form

$$(6.3) \quad \mathbb{P}[\gamma \cap A = \emptyset] = |\phi'_A(0)|^\alpha$$

for some $\alpha > 0$, see e.g. [Law05, BN16]. Now, by the domain Markov property of the SLE_κ , (6.3) gives naturally rise to a (local) martingale (similarly as in Section 5.8):

$$M_t(A) = \mathbb{P}[\gamma \cap A = \emptyset \mid \gamma[0, t]] = \mathbb{P}[\tilde{\gamma} \cap g_t(A) = \emptyset] = |\phi'_{g_t(A)}(X_t)|^\alpha,$$

where g_t is the Loewner map of the SLE_κ curve and $\tilde{\gamma}$ is an SLE_κ in $(\mathbb{H}, X_t, \infty)$ independent of $\gamma[0, t]$. Calculating the stochastic differential of $M_t(A)$ one sees that the drift term vanishes if and only if $\kappa = 8/3$ and $\alpha = 5/8$. We refer e.g. to [BB06] for the calculation.

This kind of a restriction property should hold for the scaling limit of the self-avoiding random walk. Namely, an ensemble of self-avoiding random walks is uniform, that is, every walk of the same length is counted with the same weight. Restricting to walks which avoid a region A , the measure on the set of walks should still be uniform, which is precisely the statement of the restriction property. This supports the (still open) conjecture that the $\text{SLE}_{8/3}$ is the scaling limit of self-avoiding random walks.

6.3. Brownian exterior perimeter. The *Brownian excursion measure* is a very important tool in the construction of restriction measures with Brownian loops. The Brownian excursion measure itself is a conformal restriction measure with exponent $\alpha = 1$. In this section, we investigate why the restriction property should hold and describe how to construct more general restriction measures.

The idea to define a two-dimensional Brownian excursion in \mathbb{H} from 0 to $x \in \mathbb{R}$ is to take a two-dimensional Brownian motion started from zero and conditioned to remain in the upper half-plane \mathbb{H} until escaping at x . However, such an event has probability zero (just like for the SLE_κ with $\kappa > 4$), so more care has to be taken¹⁸. To avoid difficulties, we will consider a two-dimensional Brownian motion started at $i\varepsilon$ for $\varepsilon \ll 1$ and conditioned to exit \mathbb{H} through the horizontal line $iR + \mathbb{R}$ for $R \gg 1$. By the Gambler's ruin argument, such an event has probability ε/R . Taking the limit $\varepsilon \rightarrow 0$ and $R \rightarrow \infty$, we get an excursion from 0 to ∞ (we have to look at events for which the conditioned probabilities are finite in this limit).

¹⁸Instead, a two dimensional Brownian excursion in \mathbb{H} is a process $B_t + iY_t$, where B_t is a standard one-dimensional Brownian motion and Y_t is a suitable Bessel process, see [LSW03, Law05].

Such a Brownian excursion, denoted by $(\eta_t)_{t \geq 0}$, has the restriction property. Let $A \subset \mathbb{H}$ be a hull and consider the probability $\mathbb{P}[\eta \cap A = \emptyset]$ that the Brownian excursion $\eta = \eta_{[0, \infty)}$ does not touch the hull A . To evaluate this probability, let $\mathbf{B}_t := (B_t^1, B_t^2)$ be a two-dimensional Brownian motion started at $\mathbf{B}_0 = i\varepsilon$. We should look at the probability that the process \mathbf{B}_t conditioned to exit \mathbb{H} through the horizontal line $iR + \mathbb{R}$ avoids the hull A . This probability is

$$\frac{\mathbb{P}[\{\mathbf{B} \text{ exits } \mathbb{H} \text{ through } iR + \mathbb{R}\} \cap \{\mathbf{B} \cap A = \emptyset\}]}{\mathbb{P}[\mathbf{B} \text{ exits } \mathbb{H} \text{ through } iR + \mathbb{R}]} = \frac{\mathbb{P}[\{\mathbf{B} \text{ exits } \mathbb{H} \text{ through } iR + \mathbb{R}\} \cap \{\mathbf{B} \cap A = \emptyset\}]}{\varepsilon/R}.$$

To calculate the numerator, we use conformal invariance¹⁹ of \mathbf{B} . Let $\phi_A: \mathbb{H} \setminus A \rightarrow \mathbb{H}$ be a conformal map such that $\phi_A(0) = 0$, $\phi_A(\infty) = \infty$, and $\phi'_A(\infty) = 1$. The image of the starting point $\mathbf{B}_0 = i\varepsilon$ under this map is $\phi_A(i\varepsilon) \approx i\varepsilon\phi'_A(0)$, and the horizontal line $iR + \mathbb{R}$ is mapped to almost a line slightly waving around $iR + \mathbb{R}$. Therefore, the numerator is

$$\begin{aligned} & \mathbb{P}[\{\mathbf{B} \text{ exits } \mathbb{H} \text{ through } iR + \mathbb{R}\} \cap \{\mathbf{B} \cap A = \emptyset\}] \\ & \approx \mathbb{P}[\text{a two-dimensional Brownian motion started from } i\varepsilon\phi'_A(0) \text{ exits } \mathbb{H} \text{ through } iR + \mathbb{R}] \\ & = \frac{\varepsilon\phi'_A(0)}{R}. \end{aligned}$$

We thus obtain

$$\mathbb{P}[\eta \cap A = \emptyset] = \frac{\mathbb{P}[\{\mathbf{B} \text{ exits } \mathbb{H} \text{ through } iR + \mathbb{R}\} \cap \{\mathbf{B} \cap A = \emptyset\}]}{\mathbb{P}[\mathbf{B} \text{ exits } \mathbb{H} \text{ through } iR + \mathbb{R}]} \approx \frac{\varepsilon\phi'_A(0)}{R} \frac{R}{\varepsilon} = \phi'_A(0).$$

This is the restriction property with the exponent $\alpha = 1$.

So the measure on hulls obtained by filling the regions swallowed by Brownian excursions in \mathbb{H} is a restriction measure with exponent $\alpha = 1$. For a more rigorous treatment, we refer to [LSW03, Vir03].

Brownian excursions give rise to restriction measures that are related to self avoiding walks and $\text{SLE}_{8/3}$. In fact, the hull generated by eight independent $\text{SLE}_{8/3}$ curves and the hull generated by five independent Brownian excursions have the same distribution. To see this, note that taking five independent Brownian excursions and filling the holes, one gets a restriction measure with exponent $\alpha = 1 + 1 + 1 + 1 + 1 = 5$ (by independence), and similarly, eight independent $\text{SLE}_{8/3}$ curves give rise to a restriction measure with exponent $\alpha = 5/8 + 5/8 + 5/8 + 5/8 + 5/8 + 5/8 + 5/8 + 5/8 = 5$. So we can write

$$5 \times \{\text{Brownian excursion in } \mathbb{H} \text{ from } 0 \text{ to } \infty\} = 8 \times \text{SLE}_{8/3}.$$

Benoit Mandelbrot conjectured already in 1982 that the fractal dimension of the exterior perimeter of the Brownian excursion equals $4/3$. The identification of these two restriction measures supports this conjecture: the fractal dimension of the $\text{SLE}_{8/3}$ curve is $4/3$. The mathematical proof of Mandelbrot's conjecture by Oded Schramm, Wendelin Werner, and Greg Lawler [LSW01a, LSW01c, LSW02c, LSW02a, Law02, LSW03] has been one of the main achievements in the SLE theory.

One can use the Brownian excursion measure to construct more general restriction measures as well (in fact, all of them). Indeed, for any exponent $\alpha > 5/8$ (restriction measures do not exist for $\alpha < 5/8$), the conformal restriction measure with exponent α can be constructed by adding Brownian loops to a simple SLE_κ curve in a Poissonian way (and filling the resulting holes). In this construction, $\kappa \in (0, 8/3)$ is chosen according to $\alpha(\kappa) = \frac{6-\kappa}{2\kappa}$, and the Poisson process of loops has intensity $\lambda(\kappa) = \frac{1}{2\kappa}(6-\kappa)(8-3\kappa)$. Note that the intensity exactly compensates the central charge of the corresponding CFT: $\lambda(\kappa) + c(\kappa) = 0$. We refer to the literature [Law02, LSW03, Wer03, LW04, Law05, Wer05, BB06, Wer08, Cam16] for more details about loop soups and restriction measures.

¹⁹The two-dimensional Brownian motion is conformally invariant, see e.g. [Law05], but this is not true in higher dimensions.

REFERENCES

- [Ahl79] Lars V. Ahlfors. *Complex analysis: an introduction to the theory of analytic functions of one complex variable*. International series in pure and applied mathematics. McGraw-Hill Book Co., New York, 3rd edition, 1979.
- [Bax86] Rodney J. Baxter. q colourings of the triangular lattice. *J. Phys. A*, 19(14):2821–2839, 1986.
- [Bax07] Rodney J. Baxter. *Exactly solved models in statistical mechanics*. Originally published by Academic Press, London, 1982, reprinted by Dover Publications, 3rd edition, 2007.
- [BB02] Michel Bauer and Denis Bernard. SLE $_{\kappa}$ growth processes and conformal field theories. *Phys. Lett. B*, 543(1-2):135–138, 2002.
- [BB03] Michel Bauer and Denis Bernard. Conformal field theories of stochastic Loewner evolutions. *Comm. Math. Phys.*, 239(3):493–521, 2003.
- [BB06] Michel Bauer and Denis Bernard. 2D growth processes: SLE and Loewner chains. *Phys. Rep.*, 432(3-4):115–221, 2006.
- [BBH05] M. Bauer, D. Bernard, and J. Houdayer. Dipolar stochastic Loewner evolutions. *J. Stat. Mech. Theory Exp.*, 0503:P03001, 2005.
- [BDC12] Vincent Beffara and Hugo Duminil-Copin. The self-dual point of the two-dimensional random-cluster model is critical for $q \geq 1$ one. *Probab. Th. Rel. Fields*, 153(3-4):511–542, 2012.
- [Bef04] Vincent Beffara. Hausdorff dimensions for SLE(6). *Ann. Probab.*, 32(3B):2606–2629, 2004.
- [Bef08] Vincent Beffara. The dimension of the SLE curves. *Ann. Probab.*, 36(4):1421–1452, 2008.
- [BN16] Nathanael Berestycki and James R. Norris. Lectures on Schramm-Loewner evolution. Available in <http://www.statslab.cam.ac.uk/~james/Lectures/sle.pdf>, 2016.
- [BPZ84a] A. A. Belavin, A. M. Polyakov, and A. B. Zamolodchikov. Infinite conformal symmetry in two-dimensional quantum field theory. *Nuclear Phys. B*, 241(2):333–380, 1984.
- [BPZ84b] A. A. Belavin, A. M. Polyakov, and A. B. Zamolodchikov. Infinite conformal symmetry of critical fluctuations in two-dimensions. *J. Stat. Phys.*, 34(5-6):763–774, 1984.
- [Cam16] Federico Camia. Brownian loops and conformal fields. Preprint in [arXiv:1501.04861](https://arxiv.org/abs/1501.04861), 2016.
- [Car84] John L. Cardy. Conformal invariance and surface critical behavior. *Nuclear Phys. B*, 240(4):514–532, 1984.
- [Car86] John L. Cardy. Effect of boundary conditions on the operator content of two-dimensional conformally invariant theories. *Nucl. Phys. B*, 275:200–218, 1986.
- [Car87] John L. Cardy. Conformal invariance. In *Phase transitions and critical phenomena*, volume 11, pages 55–126. Academic Press, London, 1987.
- [Car90] John L. Cardy. Conformal invariance and statistical mechanics. In E. Brézin and J. Zinn-Justin, editors, *Fields, strings, and critical phenomena, Les Houches (1988)*, volume 49. North-Holland, Amsterdam, 1990.
- [Car92] John L. Cardy. Critical percolation in finite geometries. *J. Phys. A*, 25(4):L201–206, 1992.
- [Car96] John L. Cardy. *Scaling and renormalization in statistical physics*, volume 5 of *Cambridge lecture notes in physics*. Cambridge University Press, 1996.
- [Car05] John L. Cardy. SLE for theoretical physicists. *Ann. Physics*, 318(1):81–118, 2005.
- [Car06] John L. Cardy. Boundary conformal field theory. In *Encyclopedia of Mathematical Physics*. Elsevier, 2006.
- [Car10] John L. Cardy. Conformal field theory and statistical mechanics. In J. Jacobsen and S. Ouvry, V. Pasquier, D. Serban, and L.F. Cugliandolo, editors, *Exact methods in low-dimensional statistical physics and quantum computing, Les Houches (2008)*, volume 89. Oxford University Press, 2010.
- [CDCH⁺14] Dmitry Chelkak, Hugo Duminil-Copin, Clément Hongler, Antti Kemppainen, and Stanislav Smirnov. Convergence of Ising interfaces to Schramm’s SLE curves. *C. R. Acad. Sci. Paris Sér. I Math.*, 352(2):157–161, 2014.
- [Cha10] Christophe Chatelain. Numerical study of Schramm-Loewner evolution in the random 3-state Potts model. *J. Stat. Mech. Theory Exp.*, P08004, 2010.
- [CHI15] Dmitry Chelkak, Clément Hongler, and Konstantin Izyurov. Conformal invariance of spin correlations in the planar Ising model. *Ann. Math.*, 181(3):1087–1138, 2015.
- [CI13] Dmitry Chelkak and Konstantin Izyurov. Holomorphic spinor observables in the critical Ising model. *Comm. Math. Phys.*, 322(2):303–332, 2013.
- [CN06] F. Camia and C. M. Newman. Two-dimensional critical percolation: the full scaling limit. *Comm. Math. Phys.*, 268(1):1–38, 2006.
- [CN07] F. Camia and C. M. Newman. Critical percolation exploration path and SLE(6): a proof of convergence. *Probab. Theory Related Fields*, 139(3-4):473–519, 2007.
- [Con78] John B. Conway. *Functions of one complex variable I*, volume 11 of *Graduate Texts in Mathematics*. Springer, 1978.
- [Con95] John B. Conway. *Functions of one complex variable II*, volume 159 of *Graduate Texts in Mathematics*. Springer, 1995.
- [CS12] Dmitry Chelkak and Stanislav Smirnov. Universality in the 2D Ising model and conformal invariance of fermionic observables. *Invent. Math.*, 189(3):515–580, 2012.
- [DC11] Hugo Duminil-Copin. *Phase transition in random-cluster and $O(n)$ -models*. PhD thesis, Université de Genève, 2011. Available in <https://www.unige.ch/~duminil/publi/these.pdf>.

- [DCS12] Hugo Duminil-Copin and Stanislav Smirnov. The connective constant of the honeycomb lattice equals $\sqrt{2 + \sqrt{2}}$. *Ann. of Math.*, 175(3):1653–1665, 2012.
- [DFMS97] Philippe Di Francesco, Pierre Mathieu, and David Sénéchal. *Conformal field theory*. Graduate texts in contemporary physics. Springer-Verlag, New York, 1997.
- [Dub06] Julien Dubédat. Excursion decompositions for SLE and Watts’ crossing formula. *Probab. Theory Related Fields*, 134(3):453–488, 2006.
- [Dub07] Julien Dubédat. Duality of Schramm-Loewner Evolutions. *Ann. Sci. Éc. Norm. Supér.*, 42(5):697–724, 2007.
- [Dup00] Bertrand Duplantier. Conformally invariant fractals and potential theory. *Phys. Rev. Lett.*, 84(7):1363–1367, 2000.
- [Dup04] Bertrand Duplantier. Conformal fractal geometry and boundary quantum gravity. In M. L. Lapidus and M. van Frankenhuisen, editors, *Fractal Geometry and Applications: A Jubilee of Benoît Mandelbrot*, volume 72 of *Proc. Symposia Pure Math.*, pages 365–482, Providence, R.I., 2004. American Mathematical Society.
- [Dup06] Bertrand Duplantier. Conformal random geometry. In *Mathematical Statistical Physics: Lecture Notes of the Les Houches Summer School (2005)*. Elsevier, 2006.
- [Dur96] Richard Durrett. *Stochastic calculus: a practical introduction*. Probability and stochastics series. CRC Press LLC, 1996.
- [Dur10] Richard Durrett. *Probability: theory and examples*. Cambridge University Press, 4th edition, 2010.
- [FW03] Roland Friedrich and Wendelin Werner. Conformal restriction, highest weight representations and SLE. *Comm. Math. Phys.*, 243(1):105–122, 2003.
- [GC07] Adam Gamsa and John L. Cardy. Schramm-Loewner evolution in the three-state Potts model - a numerical study. *J. Stat. Mech. Theory Exp.*, P08020, 2007.
- [Gri99] Geoffrey Grimmett. *Percolation*, volume 321 of *Grundlehren der Mathematischen Wissenschaften*. Springer-Verlag, Berlin, 2nd edition, 1999.
- [Gri09] Geoffrey Grimmett. *The random-cluster model*, volume 333 of *A series of Comprehensive Studies in Mathematics*. Springer, corrected second printing edition, 2009.
- [HKB⁺12] M. Henkel, D. Karevski, M. Bauer, C. Chatelain, and J. Jacobsen. *Conformal invariance: an introduction to loops, interfaces and stochastic Loewner evolution*. Lecture Notes in Physics. Springer-Verlag, 2012.
- [Hon06] Juha Honkonen. Lecture notes for the course “statistical physics i”. Available at <http://theory.physics.helsinki.fi/~stafyii/SFnotes.pdf>, 2006.
- [Hon10] Clément Hongler. *Conformal invariance of Ising model correlations*. PhD thesis, Université de Genève, 2010. Available in <http://www.math.columbia.edu/~hongler/thesis.pdf>.
- [Hon13] Juha Honkonen. Lecture notes for the course “statistical physics ii”. Available at <http://theory.physics.helsinki.fi/~xfiles/stafyii/14/index2013>, 2013.
- [HS13] Clément Hongler and Stanislav Smirnov. The energy density in the planar Ising model. *Acta Math.*, 211(2):191–225, 2013.
- [Izy16] Konstantin Izurov. Critical Ising interfaces in multiply-connected domains. *To appear in Probab. Th. Rel. Fields*, 2016.
- [Kad66] Leo P. Kadanoff. Scaling laws for Ising models near T_c . *Physics (Long Island City, N.Y.)*, 2(6):263–272, 1966.
- [Kad90] Leo P. Kadanoff. Scaling and universality in statistical physics. *Physica A: Statistical mechanics and its applications*, 163(1):1–14, 1990.
- [Kem16] Antti Kemppainen. *Schramm-Loewner evolution*. 2016. In preparation. Preprint available at <https://wiki.helsinki.fi/display/mathphys/kemppainen>.
- [Ken00] Richard W. Kenyon. Conformal invariance of domino tiling. *Ann. Probab.*, 28(2):759–795, 2000.
- [Ken01] Richard W. Kenyon. Dominos and the Gaussian free field. *Ann. Probab.*, 29(3):1128–1137, 2001.
- [Ken14] Richard W. Kenyon. Conformal invariance of loops in the double-dimer model. *Comm. Math. Phys.*, 326(2):477–497, 2014.
- [Kes82] Harry Kesten. *Percolation theory for mathematicians*, volume 2 of *Progress in Probability and Statistics*. Birkhäuser, Boston, Mass., 1982.
- [KN04] Wouter Kager and Bernard Nienhuis. A guide to stochastic löwner evolution and its applications. *J. Stat. Phys.*, 115(5):1149–1229, 2004.
- [KS15] Antti Kemppainen and Stanislav Smirnov. Conformal invariance of boundary touching loops of FK Ising model. Preprint in [arXiv:1509.08858](https://arxiv.org/abs/1509.08858), 2015.
- [Law02] Gregory F. Lawler. Conformal invariance, universality and the dimension of the Brownian frontier. In *Proceedings of the ICM, (Beijing, 2002)*, volume 3, pages 63–72, Beijing, 2002. Higher Education Press.
- [Law05] Gregory F. Lawler. *Conformally invariant processes in the plane*, volume 114 of *Mathematical surveys and monographs*. American Mathematical Society, 2005.
- [Loe23] Charles Loewner. Untersuchungen über schlichte konforme Abbildungen des Einheitskreises. I. *Math. Ann.*, 89:103–121, 1923.
- [LPSA94] Robert Langlands, Philippe Pouliot, and Yvan Saint-Aubin. Conformal invariance in 2D percolation. *Bull. Amer. Math. Soc.*, 90:1–61, 1994.

- [LR15] Gregory F. Lawler and Mohammad A. Rezaei. Minkowski content and natural parametrization for the Schramm-Loewner evolution. *Ann. Probab.*, 43(3):1082–1120, 2015.
- [LS11] Gregory F. Lawler and Scott Sheffield. The natural parametrization for the Schramm-Loewner evolution. *Ann. Probab.*, 39(5):1896–1937, 2011.
- [LSW01a] Gregory F. Lawler, Oded Schramm, and Wendelin Werner. The dimension of the planar Brownian frontier is $4/3$. *Math. Res. Lett.*, 8:401–411, 2001.
- [LSW01b] Gregory F. Lawler, Oded Schramm, and Wendelin Werner. Values of Brownian intersection exponents I: Half-plane exponents. *Acta Math.*, 187(2):237–273, 2001.
- [LSW01c] Gregory F. Lawler, Oded Schramm, and Wendelin Werner. Values of Brownian intersection exponents II: Plane exponents. *Acta Math.*, 187(2):275–308, 2001.
- [LSW02a] Gregory F. Lawler, Oded Schramm, and Wendelin Werner. Analyticity of intersection exponents for planar brownian motion. *Acta Math.*, 189(2):179–201, 2002.
- [LSW02b] Gregory F. Lawler, Oded Schramm, and Wendelin Werner. One-arm exponent for 2D critical percolation. *Electr. J. Probab.*, 7(2):1–13, 2002.
- [LSW02c] Gregory F. Lawler, Oded Schramm, and Wendelin Werner. Values of Brownian intersection exponents III: Two-sided exponents. *Ann. Henri Poincaré*, 38(1):109–123, 2002.
- [LSW03] Gregory F. Lawler, Oded Schramm, and Wendelin Werner. Conformal restriction: the chordal case. *J. Amer. Math. Soc.*, 16(4):917–955, 2003. (electronic).
- [LSW04] Gregory F. Lawler, Oded Schramm, and Wendelin Werner. Conformal invariance of planar loop-erased random walks and uniform spanning trees. *Ann. Probab.*, 32(1B):939–995, 2004.
- [LV16] Gregory F. Lawler and Fredrik Viklund. Convergence of loop-erased random walk in the natural parametrization. Preprint in [arXiv:1603.05203](https://arxiv.org/abs/1603.05203), 2016.
- [LW04] Gregory F. Lawler and Wendelin Werner. The Brownian loop soup. *Probab. Th. Rel. Fields*, 128(4):565–588, 2004.
- [MS12] Jason Miller and Scott Sheffield. Imaginary geometry i: Interacting SLEs. Preprint in [arXiv:1201.1496](https://arxiv.org/abs/1201.1496), 2012.
- [MS13] Jason Miller and Scott Sheffield. Quantum Loewner evolution. Preprint in [arXiv:1312.5745](https://arxiv.org/abs/1312.5745), 2013.
- [Mus10] Giuseppe Mussardo. *Statistical field theory: An Introduction to exactly solved models in statistical physics*. Oxford Graduate Texts. Oxford University Press, 2010.
- [Nie82] Bernard Nienhuis. Exact critical point and exponents of the $O(n)$ model in two dimensions. *Phys. Rev. Lett.*, 49:1062–1065, 1982.
- [Nie84] Bernard Nienhuis. Critical behavior of two-dimensional spin models and charge asymmetry in the Coulomb gas. *J. Stat. Phys.*, 34(5):731–761, 1984.
- [Nie87] Bernard Nienhuis. Coulomb gas formulation of two-dimensional phase transitions. In C. Domb and J. L. Lebowitz, editors, *Phase transitions and critical phenomena*, volume 11, pages 1–53. Academic Press, London, 1987.
- [Pol70] Alexander M. Polyakov. Conformal symmetry of critical fluctuations. *JETP Lett.*, 12(12):381–383, 1970.
- [Pol75] Alexander M. Polyakov. Interaction of goldstone particles in two dimensions. Applications to ferromagnets and massive Yang-Mills fields. *Phys. Lett. B*, 59(1):79–81, 1975.
- [Pom92] Christian Pommerenke. *Boundary behaviour of conformal maps*, volume 299 of *Grundlehren der mathematischen Wissenschaften*. Springer Verlag, Berlin Heidelberg, 1992.
- [PP66] A.Z. Patashinskii and V.L. Pokrovskii. Behavior of ordered systems near the transition point. *Soviet Physics JETP*, 23(2):292–297, 1966.
- [RS05] Steffen Rohde and Oded Schramm. Basic properties of SLE. *Ann. of Math.*, 161(2):883–924, 2005.
- [RW00a] L. C. G. Rogers and David Williams. *Diffusions, Markov processes, and martingales*, volume 1: Foundations of *Cambridge mathematical library*. Originally published by John Wiley & Sons Ltd., 1979, reprinted by Cambridge University Press, 2000.
- [RW00b] L. C. G. Rogers and David Williams. *Diffusions, Markov processes, and martingales*, volume 2: Itô calculus of *Cambridge mathematical library*. Originally published by John Wiley & Sons Ltd., 1979, reprinted by Cambridge University Press, 2000.
- [RY05] Daniel Revuz and Marc Yor. *Continuous martingales and Brownian motion*, volume 293 of *Grundlehren der mathematischen Wissenschaften*. Springer, 2005. Reprint of the 3rd ed. Berlin Heidelberg New York 1999.
- [Sch00] Oded Schramm. Scaling limits of loop-erased random walks and uniform spanning trees. *Israel J. Math.*, 118(1):221–288, 2000.
- [Sch01] Oded Schramm. A percolation formula. *Electron. Comm. Probab.*, 6:115–120, 2001. (electronic).
- [SD87] Hubert Saleur and Bertrand Duplantier. Exact determination of the percolation hull exponent in two dimensions. *Phys. Rev. Lett.*, 58:2325–2328, 1987.
- [She07] Scott Sheffield. Gaussian free field for mathematicians. *Probab. Th. Rel. Fields*, 139(3):521–541, 2007.
- [She09] Scott Sheffield. Exploration trees and conformal loop ensembles. *Duke Math. J.*, 147(1):79–129, 2009.
- [Smi01] Stanislav Smirnov. Critical percolation in the plane: conformal invariance, Cardy’s formula, scaling limits. *C. R. Acad. Sci.*, 333(3):239–244, 2001. (updated 2009, see [arXiv:0909.4499](https://arxiv.org/abs/0909.4499)).
- [Smi02] Jan Smit. *Introduction to quantum fields on a lattice*, volume 15 of *Cambridge lecture notes in physics*. Cambridge University Press, 2002.

- [Smi10] Stanislav Smirnov. Conformal invariance in random cluster models.I. Holomorphic fermions in the Ising model. *Ann. Math.*, 172(2):1435–1467, 2010.
- [SS05] Oded Schramm and Scott Sheffield. The harmonic explorer and its convergence to SLE(4). *Ann. Probab.*, 33(6):2127–2148, 2005.
- [SS09] Oded Schramm and Scott Sheffield. Contour lines of the two-dimensional discrete Gaussian free field. *Acta Math.*, 202(1):21–137, 2009.
- [SS13] Oded Schramm and Scott Sheffield. A contour line of the continuum Gaussian free field. *Probab. Theory Related Fields*, 157(1):47–80, 2013.
- [SW01] Stanislav Smirnov and Wendelin Werner. Critical exponents for two-dimensional percolation. *Math. Res. Lett.*, 8(6):729–744, 2001.
- [SW05] Oded Schramm and David B. Wilson. SLE coordinate changes. *New York J. Math.*, 11:659–669, 2005.
- [SW12] Scott Sheffield and Wendelin Werner. Conformal loop ensembles: The markovian characterization and the loop-soup construction. *Ann. Math.*, 176(3):1827–1917, 2012.
- [Uzu92] D. I. Uzunov. *Introduction to the theory of critical phenomena: mean field, fluctuations, and renormalization*. World Scientific, 1992.
- [Vir03] Balint Virag. Brownian beads. *Probab. Th. Rel. Fields*, 127(3):367–387, 2003.
- [Wat96] Gerard Watts. A crossing probability for critical percolation in two dimensions. *J.Phys. A*, 29:L363, 1996.
- [Wer03] Wendelin Werner. SLEss as boundaries of clusters of brownian loops. *C. R. Acad. Sci. Paris Sér. I Math.*, 337:481–486, 2003.
- [Wer05] Wendelin Werner. Conformal restriction and related questions. *Probability Surveys*, 2:145–190, 2005.
- [Wer06] Wendelin Werner. Some recent aspects of random conformally invariant systems. In *Mathematical Statistical Physics: Lecture Notes of the Les Houches Summer School (2005)*, chapter Course 2. Elsevier, 2006.
- [Wer08] Wendelin Werner. The conformally invariant measure on self-avoiding loops. *J. Amer. Math. Soc.*, 21(1):137–169, 2008.
- [Wil96] David B. Wilson. Generating random spanning trees more quickly than the cover time. In *Proceedings of the Twenty-eighth Annual ACM Symposium on the Theory of Computing (Philadelphia, PA, 1996)*, pages 296–303, New York, 1996. ACM.
- [WW03] Benjamin Wieland and David B. Wilson. Winding angle variance of Fortuin-Kasteleyn contours. *Phys. Review E*, 68(5):056101, 2003.
- [Zha08a] Dapeng Zhan. Duality of chordal SLE. *Invent. Math.*, 174(2):309–353, 2008.
- [Zha08b] Dapeng Zhan. Reversibility of chordal SLE. *Ann. Probab.*, 36(4):1472–1494, 2008.